

NPS ARCHIVE  
1966  
LEANE, S.

A DESIGN STUDY OF ANTENNA MODULATION  
TECHNIQUES IN REDUCED SIDELOBE LEVELS.

STEPHEN PATRICK LEANE

LIBRARY  
NAVAL POSTGRADUATE SCHOOL  
MONTEREY, CALIF. 93940

This document has been approved for public  
release and sale; its distribution is unlimited.







**A DESIGN STUDY OF ANTENNA MODULATION TECHNIQUES  
RESULTING IN REDUCED SIDELobe LEVELS**

**by**

**Stephen Patrick Leane  
Lieutenant, United States<sup>71</sup> Coast Guard  
B.S., United States Coast Guard Academy, 1961**



**Submitted in partial fulfillment  
for the degree of**

**MASTER OF SCIENCE IN COMMUNICATION ENGINEERING**

**from the**

**UNITED STATES NAVAL POSTGRADUATE SCHOOL**

**December 1966**

Thesis  
L334  
C.1

## ABSTRACT

It is desirable, for many applications, to utilize a receiving antenna system which is sensitive only to radiation from a specific direction. In order to eliminate the incoming signals from all other directions, the sidelobe strength in these regions must be significantly lower than the main beam. Time modulation was applied to certain of the antenna's parameters in an effort to reduce the sidelobe level of a linear receiving antenna array. Such factors as the effective length of the array, and the frequency and phase of the signals received by each of the individual elements were periodically varied in time. After summing the voltage contribution from each element, the resultant signal was suitably filtered and sent to the detector. Antenna field patterns were developed in mathematical terms and the experimental calculations were made on the CDC 1604 computer. For all forms of modulation investigated, it was possible to reduce the sidelobe strength by more than an order of magnitude below the unmodulated level.



## TABLE OF CONTENTS

Section	Page
1. Introduction	11
2. Fundamental Theory of Time Modulated Antenna Arrays	14
3. Model I	18
4. Model II	28
5. Model III	35
6. Model IV	41
7. Conclusions	51
8. Illustrations	53
9. Bibliography	71



## LIST OF TABLES

Table	Page
I. Calculated Field Patterns for Model I	25
II. Calculated Field Patterns for Model II	31
III. Calculated Field Patterns for Model III	38
IV. Calculated Field Patterns for Model IV	45



## LIST OF ILLUSTRATIONS

Figure	Page
1. Linear Antenna Array Used in this Study	53
2. Frequency Spectrum of $v(\theta, \phi, t)$	53
3. Static Array Field Pattern for Model I	54
4. Field Pattern for Model I with Inversely and Linearly Tapered ON Times	55
5. Field Pattern for Model I with Linearly Tapered ON Times	56
6. Field Pattern for Model I with Linearly Tapered ON Times	57
7. Field Pattern for Model I with Linearly Tapered ON Times	58
8. Field Pattern for Model I with a Binomial Distribution of ON Times	59
9. Field Pattern for Model I with a 30 db. Dolph-Tchebyscheff Distribution of ON Times	60
10. Field Pattern for Model I with a 40 db. Dolph-Tchebyscheff Distribution of ON Times	61
11. Beam Position and Beam Width as Functions of the Progressive Element Phase Delay	62
12. Antenna Array for Model II	63
13. $\sin(2\pi b_n)$ as a Function of $b_n$	63
14. Static and 40 db. Sidelobe Field Patterns for Model II	64
15. Field Patterns at the First Two Sideband Frequencies for Model II	65
16. Antenna Array for Model III	66
17. Nomogram Used for Model III	66
18. Field Patterns at the First Two Sideband Frequencies for Model III	67
19. Antenna Array for Model IV	68

# LIST OF ILLUSTRATIONS (cont.)

Figure	Page
20. Nomogram Used for Model IV	68
21. Field Pattern at the First and Third Sideband Frequencies for Model IV	69
22. Graph Used for Dolph-Tchebyscheff Calculations	70

# TABLE OF SYMBOLS AND ABBREVIATIONS

$O_n$	operator in nth feed line
$\theta$	angle measured in the plane of the receiving elements
$\phi$	angle measured out of the plane of the receiving elements
$t$	time variable
$v$	output signal voltage from the array
$\epsilon$	element radiation factor
$n$	designation of individual receiving element
$N$	total number of receiving elements
$d$	interelement spacing
$k$	propagation constant; equal to $2\pi/\lambda$
$j$	$\sqrt{-1}$
$e$	base of the natural system of logarithms (2.71828...)
$a_n$	relative excitation of the nth element
$\omega$	frequency of incoming radiation
$\lambda$	wave length of incoming radiation
$\omega_o$	modulation frequency
$m$	sideband number
$\omega_m$	frequency difference between carrier and mth sideband
$\omega'$	highest frequency component of information modulation
$T$	period of modulation
$a_{mn}$	modulated excitation coefficient
$a_{on}$	modulated excitation coefficient at the carrier frequency
$A_n$	excitation amplitude constant in nth element
$u(t)$	unit step function
$\tau_n$	ON time of nth element in Model I
db.	decibel



# TABLE OF SYMBOLS AND ABBREVIATIONS (cont.)

$G$	antenna array gain
$\psi_n$	phase difference in signal between nth element and the origin
$\rho$	progressive phase shift between adjacent elements
$b_n$	frequency controlling factor for the nth element in Model II
$k_n$	constant for the nth element in Model II; equal to $b_n \omega_0$
$\phi_n$	relative phase of signal in nth feed line of Model III
$C$	frequency constant in Model III
$K$	constant in Model III; equal to $C\omega_0$
$\phi_n(t)$	time dependent phase of signal in nth feed line in Model IV
$\phi_{An}$	phase in the nth feed line for $0 \leq t \leq \frac{T}{2}$ in Model IV
$\phi_{Bn}$	phase in the nth feed line for $\frac{T}{2} \leq t \leq T$ in Model IV
$\delta_n$	magnitude of $a_{on}$ in Model IV
$\partial_n$	phase angle of $a_{on}$ in Model IV
$Z_0$	parameter of Dolph-Tchebyscheff distribution
$I_n$	magnitude of nth Dolph-Tchebyscheff coefficient



## 1. Introduction.

The purpose of this study is to investigate various modulation techniques which, when applied to certain parameters of a linear receiving antenna array, will result in an antenna pattern with reduced sidelobe levels. By periodically varying such factors as the apparent length of the array or the excitation from the individual receiving elements, it will be shown that this objective can be realized.

With many of the more modern, highly sensitive communication and radar systems, there is a definite need for antenna configurations which possess this sidelobe property. In order to receive very weak and distant signals, such as tracking and telemetry information from space vehicles, radio frequency emissions from solar bodies, and directive, long-range communications networks, it is imperative that the sidelobe level be held to an absolute minimum. Otherwise, stronger radiation from undesired directions could enter the receiving system via the sidelobes and obscure the intended signal. In addition, low sidelobe levels are an effective countermeasure against enemy ECM jamming, as the jammer will be effective only when it is placed in the main antenna beam.

Traditionally, the designer of linear receiving arrays has but two basic variables with which to shape the antenna pattern. He can change the interelement spacing and the number of elements, and he can fix the amplitude and phase of the signal received by each element to any desired value. A combination of these techniques could, in theory, result in a large degree of sidelobe reduction. However, in actual practice, extremely small tolerances are often placed on the element spacing and excitation in order to achieve the desired degree of reduction. Meeting these narrow specifications usually proves to

be a serious problem.

In 1958, an entirely new idea in antenna design was presented by H. E. Shanks and R. W. Bickmore, engineers from the Microwave Laboratory at the Hughes Aircraft Company. They proposed a "four-dimensional" radiating system utilizing the three spatial co-ordinates with the time domain providing the additional degree of freedom.[8] Periodic modulation, when applied to any of the array parameters, was shown to result theoretically in reduced sidelobes. This design philosophy was pursued in the early 1960's by a group of engineers also from Hughes Aircraft Company under the sponsorship of the U. S. Air Force.[5, 9, 10, 11] They designed, built, and tested an antenna system whose elements were periodically switched on and off in a predetermined manner. Their experimental results have shown that the element modulation does, in fact, produce reduced sidelobes. Practically all of their effort seems to have been directed toward the on-off type of modulation. Still another group from Hughes has been engaged in developing a simultaneously-scanned, multiple-beam type of antenna using the element modulating procedure.[6, 7] Apart from these two projects, nothing has appeared in technical literature which would indicate that others are employing this technique.

In addition to achieving reduced sidelobes, there are four other properties of the receiving array which are of interest. The first three are: (1) the ability to steer the main beam, (2) the gain of the antenna, and (3) the beam width of the radiation pattern. The fourth, a factor which is particular to the modulated array, is the signal content of the sideband frequencies generated by the modulation process. While these factors are not of primary concern in this study, they do play an important part in the actual design of an antenna system. For this reason, some consideration will be given to them throughout the

report.

The body of this report is divided into three main areas. In Section 2, the basic theory of sidelobe reduction by time modulation of the array parameters will be developed. Based upon the results of this fundamental theory, four specific models, or types of modulation, will be examined in detail in Sections 3-6. The first to be investigated is the ON-OFF system developed by Hughes Aircraft Company. The remaining three types were developed by the investigator. They were chosen for the following two reasons: (1) the modulation functions could be conveniently expressed in mathematical terms, and (2) the models could be physically realized. An over-all discussion of the results obtained from the four models and the conclusions will be given in Section 7. The results of this investigation show that a significant degree of sidelobe reduction can be obtained with all four modulating techniques, provided the modulation parameters are properly chosen.

This study is theoretical in nature in that no attempt was made to physically realize any of the individual arrays. A mathematical function was assumed for each of the four models which would describe the particular type of modulation employed. Based upon these assumptions, expressions which characterize the far field pattern of the antenna arrays were developed. Next, computer programs were formulated to represent the field pattern of each model. From these programs, numerical and graphical data relating to the field patterns was supplied by the CDC 1604 computer. A large portion of the numerical data and some of the more significant graphical data have been included in this report in tabular and illustrative format.



## 2. Fundamental Theory of Time Modulated Antenna Arrays

The basic theory of time modulation as applied to sidelobe reduction in a linear receiving antenna array will be developed in this section. The derivation will be an expansion of a brief outline presented by W. H. Kummer in 1963.[5] Based upon the mathematical results of this development, specific examples of possible implementation schemes will be introduced in the following sections.

The array under consideration is depicted in Figure 1, p. 53. It consists of  $N$  identical elements equally spaced a distance  $d$  apart. The blocks labeled  $O_1, O_2, \dots, O_n$  represent operators inserted in the individual feed lines. In the unmodulated or static array they are assumed to be short circuits. With the introduction of modulation they may take the form of switches, phase shifters, voltage generators, etc., as required. The incoming plane wave of frequency  $\omega$  is assumed to originate from a distant source located at an angle  $\theta$  measured from the array axis.

If the voltages induced in each element are added together, the output signal from the array is given by[3]

$$V(\theta, \phi, t) = \epsilon(\theta, \phi) \sum_{n=0}^{N-1} a_n e^{jnkd \cos \theta} e^{j\omega t} \quad 2-1$$

where

$a_n$  is the relative excitation (amplitude and phase) of the  $n$ th element

$\epsilon(\theta, \phi)$  is the element factor ( $\phi$  is the angle measured to a point removed from the plane of Figure 1)

$k = 2\pi/\lambda$  is the propagation constant.

Now assume that the element excitations,  $a_n$ , are varied in a periodic manner with a frequency  $\omega_0 \ll \omega$ . Then, if  $a_n(t)$  is any band-limited

periodic function, it may be represented by[2]

$$a_n(t) = \frac{1}{T} \sum_{m=-M}^{+M} c_m e^{j\omega_m t} \quad 2-2$$

where

$$\omega_m = \frac{2\pi m}{T} = m\omega_0 \quad 2-3$$

and

$$c_m = \int_0^T a_n(t) e^{-j\omega_m t} dt \quad 2-4$$

If this expression for  $a_n(t)$  is substituted for  $a_n$  in equation 2-1, the array output voltage is given by

$$v(\theta, \phi, t) = \epsilon(\theta, \phi) \sum_{n=0}^{N-1} \left( \frac{1}{T} \sum_{m=-M}^{+M} c_m e^{j\omega_m t} \right) e^{jnKd \cos \theta} e^{j\omega t}$$

$$v(\theta, \phi, t) = \epsilon(\theta, \phi) \sum_{m=-M}^{+M} e^{j(\omega + m\omega_0)t} \sum_{n=0}^{N-1} a_{mn} e^{jnKd \cos \theta} \quad 2-5$$

where

$$a_{mn} = \frac{1}{T} c_m = \frac{1}{T} \int_0^T a_n(t) e^{-j\omega_m t} dt \quad 2-6$$

The function  $a_{mn}$  is referred to as the modulated excitation coefficient in this investigation.

Referring to equation 2-5, the frequency spectrum of the array voltage consists of  $2M + 1$  lines resulting from the modulation of the receiving elements. These lines are centered around  $\omega$  and are spaced  $\omega_0$  apart as shown in Figure 2, p. 53. Also appearing in the spectrum are the sideband frequencies containing the information impressed upon the

carrier at the transmitting source. Assuming that the highest frequency component of the information modulation is  $\omega'$ , the value of  $\omega_0$  must be equal to or greater than  $2\omega'$  in order to preserve the information content of the original signal. This requirement is a direct result of the sampling theorem applied to a slightly different physical situation. Also included in Figure 2, is a representation of a band-pass filter extending from  $(\omega-\omega')$  to  $(\omega+\omega')$ . If the signal is passed through this filter prior to detection, the resulting signal voltage may be obtained from equation 2-5 by setting  $m = 0$ .

$$V(\theta, \phi, t) = E(\theta, \phi) e^{j\omega t} \sum_{n=0}^{N-1} a_{on} e^{jnkd \cos \theta} \quad 2-7$$

where

$$a_{on} = \frac{1}{T} \int_0^T a_n(t) dt \quad 2-8$$

The radiation pattern which results from the filtered signal is simply the pattern of an array with the element excitation coefficients equal to the time averages of the periodically varying excitation coefficients. That is, the relative element excitations have been changed from  $a_n$  to the modulated excitation coefficient  $a_{on}$ . By properly choosing the form of the modulation, significant sidelobe reduction may be achieved. As expected, some time varying excitation functions tend to have the opposite effect of increasing the sidelobe response.

Four specific forms of modulation which might be employed in an effort to reduce the sidelobe level in a linear receiving array are investigated in the next four sections. A number of other modulation techniques were analyzed for possible use; however, the mathematical results differed only slightly from those included in this report. In

addition, they were felt to be more difficult to actually implement into the antenna system.

For each model, an assumption is made as to the nature of the operators in the various feed lines. From this assumption, an expression for the modulated excitation coefficient is developed based upon the theory which was derived in this section. This leads directly into a mathematical representation of the filtered signal entering the detector.



### 3. Model I

Probably the simplest form of periodic modulation which can be applied to the receiving array is an ON-OFF binary switching sequence. The operators in the individual feed lines are electronic switches which have been programmed to open and close in a periodic manner. When a particular switch is open, no contribution to the total array signal is made by the respective element. With the switch closed, the signal received by the element is allowed to pass unaltered to the array output. This form of modulation has actually been applied to a slotted receiving antenna array with excellent results.[5, 9, 10, 11]

The modulation function may be represented mathematically by

$$a_n(t) = A_n [U(t) - U(t - \tau_n)] \quad 3-1$$

where

$A_n$  is an amplitude constant

$U(t)$  is the unit step function

$\tau_n$  is the ON time per period of the nth element ( $0 \leq \tau_n \leq T$ ).

Then, from equation 2-8,

$$\begin{aligned} a_{on} &= \frac{1}{T} \int_0^T a_n(t) dt \\ &= \frac{1}{T} \int_0^T A_n [U(t) - U(t - \tau_n)] dt \\ a_{on} &= \frac{A_n \tau_n}{T} \end{aligned} \quad 3-2$$

Using this result in equation 2-7,

$$\begin{aligned} v(\theta, \phi, t) &= \epsilon(\theta, \phi) e^{j\omega t} \sum_{n=0}^{N-1} a_{on} e^{jnKd \cos \theta} \\ &= \epsilon(\theta, \phi) e^{j\omega t} \sum_{n=0}^{N-1} \frac{\tau_n}{T} A_n e^{jnKd \cos \theta} \end{aligned} \quad 3-3$$



An examination of equation 3-3 reveals that in addition to an element amplitude factor,  $A_n$ , the output signal from the array is dependent upon a variable time parameter,  $\tau_n/T$ . In the unmodulated case, the signal voltage was dependent upon three receiver parameters: (1) number of elements, (2) element spacing, and (3) element excitation. A fourth variable, time, has been added by the modulation process. A great deal of study has been directed toward determining the received signal as a function of the excitation, spacing, and number of elements. Attention will now be given to the received signal's dependence upon time modulation of the individual elements.

With four parameters in the general case, the significance of the applied modulation could very quickly become obscured if they were all allowed to vary throughout this study. To reduce the problem, certain of the parameters have been set constant, both for this model and the three which follow. The five normalizing assumptions chosen for this investigation are:

1. The number of individual receiving elements,  $N$ , is equal to eight.
2. The interelement spacing,  $d$ , is constant at  $\lambda/2$ .
3. The element factor,  $\epsilon(\theta, \phi)$ , is equal to one corresponding to isotropic receiving elements.
4. The individual element excitation gain,  $A_n$ , is equal to one.
5. The period of the modulating signal,  $T$ , is one unit of time.

Thus, for the binary switching form of modulation used in Model I, the output signal from the array is dependent solely upon the ON times,  $\tau_n$ , of the individual elements. This dependence was investigated using a number of standard distributions. Because of the fact that the variable  $\tau_n$  is quite simple from both a mathematical and a physical viewpoint, the

distributions actually employed are examined in some detail. In the models which follow, the parameter distributions are not as clearly visualized; however, they are based largely upon the distribution criterians developed for  $\tau_n$ .

The static, or unmodulated, array pattern was determined by using a uniform distribution for  $\tau_n$ . All of the values of  $\tau_n$  were set equal to one which corresponds to each element being ON at all times. The resulting array pattern, shown in Figure 3, p. 54, provides a standard of comparison for future modulating techniques. As was expected from a linear array of this type, three sidelobes were formed in the first quadrant with amplitudes of 12.8, 16.4, and 17.9 db. below the main beam. Since the array pattern is the Fourier transform of the element excitation, the minimum theoretical value for the first sidelobe is -13.5 db. for a uniform distribution, regardless of the number of elements. All of the antenna pattern figures are drawn for a single quadrant. This same pattern is present in all four quadrants by the very nature of this antenna. The one exception to the above statement is in the case of main lobe steering which will be covered later in this section.

A linearly tapered distribution for  $\tau_n$  was investigated using various degrees of taper. It was discovered very quickly that the inversely tapered distribution shown in Figure 4, p. 55, was ineffective in reducing the sidelobe level. The first sidelobe was only 5.7 db. below the main beam. The field pattern resulting from the same degree of taper applied to the array in the opposite direction is shown in Figure 5, p. 56. At the beginning of a modulation cycle, time  $t=0$ , all of the elements were ON and contributing to the array output. The outer two were turned OFF at time  $t = \tau_1 = \tau_8$ ; the next outer two elements were switched OFF at time  $t = \tau_2 = \tau_7$ ; the next two at  $t = \tau_3 = \tau_6$ ; the center two

elements were left ON for the entire period, T. At time  $t=T$ , all of the elements were again switched ON and the process was repeated. Figures 6 and 7, pp. 57 & 58, show the antenna pattern for two additional degrees of linear taper applied to  $\tau_n$ . Both showed a marked improvement in sidelobe reduction over the static pattern.

The values of  $\tau_n$  were then selected in accordance with the binomial distribution. The receiving pattern, shown in Figure 8, p. 59, indicates that no sidelobes were formed. The disadvantage of this pattern is the very wide beam width of 28.4 degrees.

Finally, two of the Dolph-Tchebyscheff distributions were applied to  $\tau_n$ . The important features of these distributions and some sample calculations are presented in the Appendix. The two distributions actually used were the -30 db. and -40 db. sidelobe coefficients. Figures 9 and 10, pp. 60 & 61, show the antenna pattern for these two cases which are in close agreement with the expected values.

In the mathematical development of the fundamental theory presented in Section 2, sidebands were formed around the carrier frequency as a result of the modulation which was applied to the array elements. Is it possible that a significant portion of the received signal falls in these sidebands, thereby reducing the strength of the desired signal at the carrier frequency? From equation 2-6, the modulated excitation coefficient is defined as follows:

$$a_{mn} = \frac{1}{T} \int_0^T a_n(t) e^{-j\omega_m t} dt \quad 3-4$$

For the type of modulation employed in Model I,

$$a_n(t) = A_n [U(t) - U(t - \tau_n)] \quad 3-5$$



It follows that

$$\begin{aligned}
 a_{mn} &= \frac{1}{T} \int_0^T A_n [U(t) - U(t - \tau_n)] e^{-j\omega_m t} dt \\
 &= \frac{A_n}{T} \int_0^{\tau_n} e^{-j\omega_m t} dt \\
 &= \frac{A_n}{T} \left( \frac{e^{-j\omega_m t}}{-j\omega_m} \right) \Big|_0^{\tau_n} \\
 &= \frac{A_n}{T} \left( \frac{e^{-j\omega_m \tau_n} - 1}{-j\omega_m} \right) \\
 &= \frac{2 A_n}{\omega_m T} e^{-j\omega_m \tau_n / 2} \sin \left( \frac{\omega_m \tau_n}{2} \right) \\
 &= \frac{A_n}{\pi m} \left[ \cos \left( \frac{\omega_m \tau_n}{2} \right) - j \sin \left( \frac{\omega_m \tau_n}{2} \right) \right] \sin \left( \frac{\omega_m \tau_n}{2} \right) \\
 &= \frac{A_n}{2\pi m} \left[ \sin \omega_m \tau_n - j(1 - \cos \omega_m \tau_n) \right] \\
 a_{mn} &= \frac{A_n}{2\pi m} \left[ \sin 2\pi m \frac{\tau_n}{T} - j(1 - \cos 2\pi m \frac{\tau_n}{T}) \right] \quad 3-6
 \end{aligned}$$

Note that by use of L'Hospital's rule, this function will reduce to

$$a_{0n} = A_n \frac{\tau_n}{T}$$

at the carrier frequency as determined by equation 3-2.

The unfiltered signal from the receiving array is

$$\begin{aligned}
 v(\theta, \phi, t) &= \epsilon(\theta, \phi) \sum_{m=-M}^{+M} e^{j(\omega + m\omega_0)t} \sum_{n=0}^{N-1} \frac{A_n}{2\pi m} \cdot \\
 &\quad \cdot \left[ \sin 2\pi m \frac{\tau_n}{T} - j(1 - \cos 2\pi m \frac{\tau_n}{T}) \right] e^{jnKd \cos \theta} \quad 3-7
 \end{aligned}$$

Since a great deal of study has been made of the sideband signals for Model I, the detailed results are not presented here.[9, 10, 11] In general, depending upon the particular distribution employed for  $\tau_n$ , the level of the maximum signal in the first sideband is between 12 and 21 db. below the peak signal at the carrier frequency. Higher order sidebands are even less significant. The total signal power which has been converted into all of the sidebands represents a loss of less than 0.5 db. This is quite acceptable in view of the sizable reduction in side-lobe level.

Because all of the elements are not contributing to the received signal at all times, the antenna gain of the modulated array is less than that of the unmodulated array. It has been shown that the ratio of modulated array gain to static array gain is given by[5]

$$\frac{G_{\text{mod.}}}{G_{\text{stat.}}} = \frac{\sum_{n=0}^{N-1} |a_{on}|^2}{\sum_{n=0}^{N-1} |A_n|^2} = \frac{\sum_{n=0}^{N-1} |A_n \frac{\tau_n}{T}|^2}{\sum_{n=0}^{N-1} |A_n|^2}$$

3-8

where

$A_n$  is the relative excitation of the nth element

$\tau_n$  is the ON time of the nth element

T is the period of modulation.

For the distributions investigated for Model I with  $A_n = 1$  and  $T = 1$ , the gain of the modulated array was reduced by about 3 to 4 db. below the unmodulated array. If, in addition to array modulation, relative element excitations are also tapered, the gain is reduced by less than 1 db. Therefore, it is desirable in practice to achieve as large

a degree of sidelobe reduction as possible using amplitude taper prior to applying the element modulation. A summary of the results for Model I with different values of the parameter,  $\tau_n$ , is given in Table I.

In concluding the study of binary ON-OFF modulation, it was desirable to determine the effect of this modulation upon the ability to steer the main beam. This is certainly a desirable feature which would add to the versatility of the antenna. With all of the element excitations in phase, the phase difference between the  $n$ th element and the origin,  $n = 0$ , is equal to

$$\psi_n = n K d \cos \theta \quad 3-9$$

where

$\psi_n$  = phase difference in signal between elements 0 and  $n$

$k = 2\pi/\lambda$

$d$  = element spacing

$\theta$  = direction in space measured from the line of the array

If it is now assumed that a progressive phase shift equal to  $\rho$  is applied between adjacent elements, the relative phase of the signal in the  $n$ th element with respect to the origin is

$$\begin{aligned} \psi_n &= n K d \cos \theta + n \rho \\ \psi_n &= n (K d \cos \theta + \rho) \end{aligned} \quad 3-10$$

The far field modulated pattern at the carrier frequency now becomes

$$V(\theta, \phi, t) = E(\theta, \phi) e^{j\omega t} \sum_{n=0}^{N-1} A_n \frac{\tau_n}{T} e^{jn(Kd \cos \theta + \rho)} \quad 3-11$$

TABLE I  
CALCULATED FIELD PATTERNS FOR MODEL I

Type of Modulation	$\tau_1, \tau_8$	$\tau_2, \tau_7$	$\tau_3, \tau_6$	$\tau_4, \tau_5$	Beam Width (deg.)	1st Side-lobe (db.)	2nd Side-lobe (db.)	3rd Side-lobe (db.)	Gain w/r/t Static (db.)
Static	1.0	1.0	1.0	1.0	17.5	-12.8	-16.4	-17.9	0.0
Linear Taper	1.0	0.75	0.50	0.25	14.6	-5.7	-11.9	-12.6	-3.30
Linear Taper	0.7	0.8	0.9	1.0	18.6	-16.3	-18.4	-20.4	-1.35
Linear Taper	0.4	0.6	0.8	1.0	20.8	-24.7	-22.1	-25.8	-2.73
Linear Taper	0.25	0.50	0.75	1.0	23.0	-37.1	-25.7	-33.4	-3.30
Linear Taper	0.1	0.4	0.7	1.0	26.4	-51.3	-30.3	—	-3.82
Binomial	0.029	0.20	0.60	1.0	28.4	-98.5	—	—	-4.47

TABLE I (continued)

Type of Modulation	$\tau_1, \tau_8$	$\tau_2, \tau_7$	$\tau_3, \tau_6$	$\tau_4, \tau_5$	Beam Width (deg.)	1st Side-lobe (db.)	2nd Side-lobe (db.)	3rd Side-lobe (db.)	Gain w/r/t Static (db.)
Misc.	0.12	0.30	0.67	1.0	27.0	-33.3	—	—	-4.11
Misc.	0.20	0.43	0.75	1.0	24.2	-30.6	-31.9	—	-3.50
Misc.	0.15	0.34	0.70	1.0	26.0	-31.5	—	—	-3.90
26 db. Dolph-Tcheby.	0.322	0.548	0.839	1.0	22.0	-27.4	-28.0	-26.3	-2.88
30 db. Dolph-Tcheby.	0.268	0.528	0.819	1.0	22.6	-29.0	-30.0	-29.9	-2.96
40 db. Dolph-Tcheby.	0.144	0.413	0.755	1.0	25.2	-41.9	-39.7	-40.1	-3.56



The position of the main beam and the beam width as a function of positive values of  $\rho$  are shown in Figure 11, p. 62. The main beam was formed by applying a 40 db. Dolph-Tchebyscheff distribution for  $\tau_n$ . Negative values of  $\rho$  will produce the same steering effects in the opposite direction. Main beam steering can be accomplished in the modulated array in exactly the same manner as the static array. The sidelobe level remains approximately 40 db. below the main beam as the beam is steered to different positions up to about  $125^\circ$  corresponding to  $\rho = 100$ . For further increases of  $\rho$ , the beam begins to widen on one side and becomes distorted. This rather sharp increase in beam width is quite evident from Figure 11. As a result, it appears that the beam may be steered through an arc of about  $70^\circ$  centered around the broadside position without any harmful effects. Further attempts to move the main beam result in a sharply increased beam width, a distorted beam shape, and an increased sidelobe level.

While this was the only type of modulation in which the beam steering capability was thoroughly investigated, the development indicates that the same results will hold true using other forms of modulation. This is due to the location of the progressive phase delay factor in the general form of the field equation. It does not appear as a multiplying factor but as an exponent along with the expression  $(nkd \cos \theta)$ . This will be true regardless of the form which the modulation takes and as such, is independent of the modulation.

#### 4. Model II

A second type of array modulation is produced by varying the signals received by the individual elements in accordance with locally generated sinusoidal signals of different frequencies and amplitudes placed in each feed line. This form of modulation was developed for two reasons:

(1) the mathematical convenience of analyzing the functions, and (2) the relative simplicity of physically realizing the system. Each feed line contains a sinusoidal voltage generator of frequency  $b_n \omega_0$ , and a non-linear modulation device as shown in Figure 12, p. 63. By properly controlling the value of  $b_n$  in each feed line, significant sidelobe reduction is possible. The array modulation function can be represented by

$$a_n(t) = A_n K_n \cos K_n t \quad 4-1$$

where

$A_n$  is an amplitude factor

$$K_n = b_n \omega_0$$

$$\omega_0 \ll \omega$$

Then, from equation 2-8,

$$\begin{aligned} a_{on} &= \frac{1}{T} \int_0^T a_n(t) dt \\ &= \frac{1}{T} \int_0^T A_n K_n \cos K_n t dt \\ &= \frac{A_n K_n}{T} \left( \frac{1}{K_n} \right) \sin K_n t \Big|_0^T \end{aligned}$$

$$a_{on} = \frac{A_n}{T} \sin K_n T \quad 4-2$$

but since

$$K_n = b_n \omega_0 = \frac{2\pi b_n}{T}$$

it follows that

$$a_{on} = \frac{A_n}{T} \sin 2\pi b_n \quad 4-3$$

The filtered signal from the array is

$$v(\theta, \phi, t) = E(\theta, \phi) e^{j\omega t} \sum_{n=0}^{N-1} \frac{A_n}{T} \sin(2\pi b_n) e^{jnKd \cos \theta} \quad 4-4$$

The modulated excitation coefficient for Model II given by equation 4-2 is

$$a_{on} = \frac{A_n}{T} \sin 2\pi b_n$$

which reduces to

$$a_{on} = \sin 2\pi b_n \quad 4-5$$

when the normalizing assumptions,  $A_n = 1$  and  $T = 1$ , are applied. As a result, the only variable remaining is  $b_n$ . The same distributions which were used to describe  $\tau_n$  in Model I may now be applied to the quantity  $\sin(2\pi b_n)$ . The magnitude of  $\sin(2\pi b_n)$  as a function of  $b_n$  is shown in Figure 13, p. 63. By knowing the desired magnitudes of the modulated excitation coefficients, values of  $b_n$  may be determined directly from Figure 13. For example, the coefficients of the 40 db. Dolph-Tchebyscheff distribution are 0.144, 0.413, 0.755, and 1.000. The corresponding values of  $b_n$  are 0.02305, 0.0678, 0.1365, and 0.250. Another set of values exist for  $b_n$  in the interval  $(0.25 \leq b_n \leq 0.50)$  which would produce the same

degree of sidelobe reduction. Since the original expression for the array modulation function was

$$a_n(t) = A_n b_n \omega_0 \cos b_n \omega_0 t$$

the smaller set of values for  $b_n$  was chosen in order to reduce the magnitude of the modulation function.

Figure 14, p. 64, shows the antenna patterns of the static array and the 40 db. Dolph-Tchebyscheff distribution applied to  $\sin(2\pi b_n)$ . The sidelobe reduction was quite significant. A number of other values of  $b_n$  were examined and the results are tabulated in Table II.

The introduction of modulation into the system results in some of the signal power distributed in the sideband frequencies

$$\omega + m\omega_0 ; m = \pm 1, \pm 2, \dots, \pm M$$

These frequencies should be filtered out prior to detection; however, it is desirable to determine just how much they detract from the signal at the carrier frequency. From equation 2-6, the general expression for the modulated excitation coefficient is

$$a_{mn} = \frac{1}{T} \int_0^T a_n(t) e^{-j\omega_m t} dt$$

4-6

where

$$a_n(t) = A_n K_n \cos K_n t$$

$$\omega_m = m\omega_0 = \frac{2\pi m}{T} ; m = 0, \pm 1, \pm 2, \dots, \pm M$$

$$K_n = b_n \omega_0$$

Thus,

$$a_{mn} = \frac{A_n K_n}{T} \int_0^T \cos(K_n t) e^{-j\omega_m t} dt$$



TABLE II  
CALCULATED FIELD PATTERNS FOR MODEL II

Type of Modulation	$b_1, b_8$	$b_2, b_7$	$b_3, b_6$	$b_4, b_5$	Beam Width (deg.)	1st Side-lobe (db.)	2nd Side-lobe (db.)	3rd Side-lobe (db.)	Gain w/r/t Static (db.)
Static	0.25	0.25	0.25	0.25	17.5	-12.8	-16.4	-17.9	0.0
Misc.	0.100	0.125	0.167	0.25	19.2	-18.9	-19.5	-21.2	-1.85
Misc.	0.056	0.111	0.167	0.222	21.4	-21.7	-27.5	-29.9	-2.50
Misc.	0.077	0.100	0.143	0.250	20.2	-24.7	-19.8	-22.8	-2.64
Misc.	0.087	0.111	0.154	0.250	20.0	-21.4	-19.8	-22.0	-2.30
Misc.	0.063	0.083	0.125	0.250	21.4	-39.6	-19.3	-24.3	-3.21
Misc.	0.057	0.077	0.118	0.250	22.0	-18.9	-25.1	—	-3.48
30 db. Dolph-Tcheby.	0.0432	0.0887	0.1528	0.250	22.6	-29.0	-30.0	-29.9	-2.96
40 db. Dolph-Tcheby.	0.0231	0.0678	0.1365	0.250	25.2	-41.5	-40.1	-39.8	-3.56

$$\begin{aligned}
a_{mn} &= \left( \frac{A_n K_n}{T} \right) \frac{e^{-j\omega_m t}}{K_n^2 - \omega_m^2} \left( K_n \sin K_n t - j\omega_m \cos K_n t \right) \Big|_0^T \\
&= \left( \frac{A_n K_n}{T} \right) \left[ \frac{e^{-j\omega_m T}}{K_n^2 - \omega_m^2} (K_n \sin K_n T - j\omega_m \cos K_n T) - \frac{1}{K_n^2 - \omega_m^2} (-j\omega_m) \right] \\
&= \frac{A_n K_n}{T(K_n^2 - \omega_m^2)} \left[ e^{-j2\pi m} (K_n \sin K_n T - j\omega_m \cos K_n T) + j\omega_m \right] \\
&= \frac{A_n K_n}{T(K_n^2 - \omega_m^2)} \left[ (\cancel{\cos 2\pi m} - j \cancel{\sin 2\pi m}) (K_n \sin K_n T - j\omega_m \cos K_n T) + j\omega_m \right] \\
&= \frac{A_n K_n}{T(K_n^2 - \omega_m^2)} \left[ K_n \sin 2\pi b_n + j\omega_m (1 - \cos 2\pi b_n) \right] \\
&= \frac{A_n b_n \omega_0}{T\omega_0^2 (b_n^2 - m^2)} \left[ b_n \omega_0 \sin 2\pi b_n + j m \omega_0 (1 - \cos 2\pi b_n) \right] \\
a_{mn} &= \frac{A_n b_n}{T(b_n^2 - m^2)} \left[ b_n \sin 2\pi b_n + j m (1 - \cos 2\pi b_n) \right] \quad 4-7
\end{aligned}$$

The unfiltered signal from the receiving array is then

$$\begin{aligned}
v(\theta, \phi, t) &= \epsilon(\theta, \phi) \sum_{m=-M}^{+M} e^{j(\omega + m\omega_b)t} \sum_{n=0}^{N-1} \frac{A_n b_n}{T(b_n^2 - m^2)} \cdot \\
&\quad \cdot \left[ b_n \sin 2\pi b_n + j m (1 - \cos 2\pi b_n) \right] e^{jn K_d \cos \theta} \quad 4-8
\end{aligned}$$

In order to obtain a feeling for the magnitudes which result from equation 4-8, the carrier plus the first two sideband signals were determined for a 40 db. Dolph-Tchebyscheff distribution applied to  $\sin(2\pi b_n)$ . The results are shown graphically in Figure 15, p. 65. For radiation received from a direction along the boresight axis, the first and second sideband signals are down 16.9 and 23.5 db., respectively, from the carrier signal. However, for all incoming radiations in the interval  $(32.5^\circ \leq \theta \leq 65.5^\circ)$ , both of the first two sideband levels are higher than the signal at the carrier frequency. It is evident from these results that the filter must possess a sharp cutoff characteristic about the carrier frequency in order to realize the desired degree of sidelobe reduction.

Following a similar line of reasoning which was used to determine equation 3-8, the ratio of the modulated antenna gain to the static array gain is equal to

$$\frac{G_{\text{mod.}}}{G_{\text{stat.}}} = \frac{\sum_{n=0}^{N-1} |a_{on}|^2}{\sum_{n=0}^{N-1} |A_n|^2}$$

$$\frac{G_{\text{mod.}}}{G_{\text{stat.}}} = \frac{\sum_{n=0}^{N-1} \left| A_n \sin \frac{2\pi b_n}{T} \right|^2}{\sum_{n=0}^{N-1} |A_n|^2}$$

4-9

where

$A_n$  is the relative excitation of the nth element

$b_n$  is the modulation parameter

$T$  is the period of modulation

In general, the modulated antenna gain was found to be 2 to 4 db. below the unmodulated gain. This gain reduction is included in Table II, p. 31.



## 5. Model III

A variation of the technique used in Model II would consist of modulating the signals from the individual elements with locally generated sinusoidal signals of constant frequency,  $C \omega_0$ , but of varying phase,  $\phi_n$ . This system would require only one generator which would be connected to the various feed lines through phase shifting networks or delay lines. The resulting signal would be combined with the received signal in each feed line modulating element as shown in Figure 16, p. 66. Sidelobe reduction is achieved by introducing into each line the proper degree of phase shift. Mathematically, the array modulation takes the form

$$a_n(t) = A_n K \cos(Kt + \phi_n)$$

5-1

where

$$K = C \omega_0$$

$$\omega_0 \ll \omega$$

The modulated excitation coefficient is equal to

$$a_{on} = \frac{1}{T} \int_0^T A_n K \cos(Kt + \phi_n) dt$$

$$= \frac{A_n K}{T} \left( \frac{1}{K} \right) \sin(Kt + \phi_n) \Big|_0^T$$

$$= \frac{A_n}{T} [\sin(KT + \phi_n) - \sin \phi_n]$$

but since

$$K = C \omega_0 = \frac{2\pi C}{T}$$

it follows that

$$a_{0n} = \frac{A_n}{T} \left[ \sin(2\pi C + \phi_n) - \sin \phi_n \right]$$

$$a_{0n} = \frac{2A_n}{T} \sin(\pi C) \cos(\pi C + \phi_n) \quad 5-2$$

the signal entering the detector is

$$v(\theta, \phi, t) = E(\theta, \phi) e^{j\omega t} \sum_{n=0}^{N-1} \frac{2A_n}{T} \cdot \sin(\pi C) \cos(\pi C + \phi_n) e^{jnKd \cos \theta} \quad 5-3$$

From equation 5-2, the expression for the normalized modulated excitation coefficient at the carrier frequency is

$$a_{0n} = 2 \sin(\pi C) \cos(\pi C + \phi_n) \quad 5-4$$

This expression differs from those given for Models I and II in that it is now a function of two variables: (1) the frequency of the sinusoidal feed line signal, and (2) the phase relationships which exist between these sinusoids. For integral values of  $C$ , the modulated excitation coefficient is equal to zero, regardless of the phase relationships. A plot of the expression  $[2 \sin(\pi C) \cos(\pi C + \phi)]$  as a function of  $\phi$  for various values of  $C$  is given in Figure 17, p. 66. Once a particular value of  $C$  is chosen, the desired amplitudes of the coefficients are obtained by properly selecting values for  $\phi_n$ . This is a very practical method for determining the coefficient values. For example, the amplitude coefficients for a 40 db. Dolph-Tchebyscheff distribution

have previously been determined to be 0.144, 0.413, 0.755, and 1.000.

To obtain these coefficients with a value of  $C = 0.25$ , the relative phase of the sinusoidal modulation is  $39.25^\circ$ ,  $28.0^\circ$ ,  $12.75^\circ$ , and  $0.0^\circ$ .

These values can be obtained with phase shifting networks or delay lines.

Some computed results obtained by varying  $C$  and  $\phi_n$  are given in Table III.

Employing some of the techniques used in Models I and II, an analysis of the signal content in the sidebands generated by the modulation process was developed. The general form of the modulated excitation coefficient is given by

$$a_{mn} = \frac{1}{T} \int_0^T a_n(t) e^{-j\omega_m t} dt$$

5-5

where

$$a_n(t) = A_n K \cos(Kt + \phi_n)$$

$$K = C\omega_0$$

$$\omega_m = m\omega_0 = \frac{2\pi m}{T}; m = 0, \pm 1, \pm 2, \dots, \pm M$$

Therefore,

$$\begin{aligned} a_{mn} &= \frac{A_n K}{T} \int_0^T \cos(Kt + \phi_n) e^{-j\omega_m t} dt \\ &= \frac{A_n K}{T} \int_0^T (\cos Kt \cos \phi_n - \sin Kt \sin \phi_n) e^{-j\omega_m t} dt \\ &= \frac{A_n K}{T} \left[ \cos \phi_n \left( \frac{e^{-j\omega_m t}}{K^2 - \omega_m^2} \right) (K \sin Kt - j\omega_m \cos Kt) \right. \\ &\quad \left. + \sin \phi_n \left( \frac{e^{-j\omega_m t}}{K^2 - \omega_m^2} \right) (K \cos Kt + j\omega_m \sin Kt) \right] \Big|_0^T \end{aligned}$$

TABLE III

## CALCULATED FIELD PATTERNS FOR MODEL III

Type of Modulation	C	$\phi_1, \phi_8$ (deg.)	$\phi_2, \phi_7$ (deg.)	$\phi_3, \phi_6$ (deg.)	$\phi_4, \phi_5$ (deg.)	Beam Width (deg.)	1st Side- lobe (db.)	2nd Side- lobe (db.)	3rd Side- lobe (db.)	Gain w/r/t Static (db.)
Static	0.25	0.0	0.0	0.0	0.0	17.5	-12.8	-16.4	-17.9	0.0
Misc.	0.25	40.0	30.0	20.0	10.0	25.0	-39.2	-30.6	—	-5.36
Misc.	0.25	30.0	20.0	10.0	0.0	21.2	-25.0	-23.7	-27.4	-2.70
Misc.	0.25	15.0	10.0	5.0	0.0	18.6	-16.1	-18.5	-20.4	-1.27
Misc.	0.25	45.0	30.0	15.0	0.0	29.2	-26.7	-25.3	—	-3.89
40 db. Dolph- Tcheby.	0.25	39.25	28.0	12.75	0.0	25.3	-41.1	-39.7	-41.2	-3.56

$$a_{mn} = \frac{A_n K}{T(K^2 - \omega_m^2)} \left\{ \cos \phi_n \left[ e^{-j\omega_m T} (K \sin KT - j\omega_m \cos KT) + j\omega_m \right] \right. \\ \left. + \sin \phi_n \left[ e^{-j\omega_m T} (K \cos KT + j\omega_m \sin KT) - K \right] \right\}$$

but since  $e^{-j\omega_m T} = e^{-j2\pi m} = \cos 2\pi m - j \sin 2\pi m = 1$

$$a_{mn} = \frac{A_n C \omega_0}{T \omega_0^2 (C^2 - m^2)} \left\{ \cos \phi_n \left[ C \omega_0 \sin 2\pi C + j m \omega_0 (1 - \cos 2\pi C) \right] \right. \\ \left. + \sin \phi_n \left[ C \omega_0 (\cos 2\pi C - 1) + j m \omega_0 \sin 2\pi C \right] \right\}$$

$$= \frac{A_n C}{T(C^2 - m^2)} \left[ C (\cos \phi_n \sin 2\pi C + \sin \phi_n \cos 2\pi C - \sin \phi_n) \right. \\ \left. - j m (-\sin \phi_n \sin 2\pi C + \cos \phi_n \cos 2\pi C - \cos \phi_n) \right]$$

$$a_{mn} = \frac{A_n C}{T(C^2 - m^2)} \left\{ C [\sin(2\pi C + \phi_n) - \sin \phi_n] \right. \\ \left. - j m [\cos(2\pi C + \phi_n) - \cos \phi_n] \right\}$$



The unfiltered signal from the antenna array is then

$$V(\theta, \phi, t) = E(\theta, \phi) \sum_{m=-M}^{+M} e^{j(\omega + m\omega_0)t} \sum_{n=0}^{N-1} \frac{A_n C}{T(C^2 - m^2)} e^{jnKd \cos \theta} \quad \bullet$$

$$\bullet \left\{ C [\sin(2\pi C + \phi_n) - \sin \phi_n] - jm [\cos(2\pi C + \phi_n) - \cos \phi_n] \right\} \quad 5-7$$

Figure 18, p. 67, shows the signals at the carrier plus the first two sideband frequencies for a 40 db. Dolph-Tchebyscheff coefficient distribution. This figure points out once again the necessity for employing a filter with sharp frequency cutoff characteristics. The two sideband signals are greater than the desired signal for values of  $\theta$  less than about  $70^\circ$ . If these signals were permitted to reach the detector, the effort expended in achieving -40 db. sidelobes would have been wasted.

The ratio of the modulated antenna gain to that of the static array at the carrier frequency is given by

$$\begin{aligned} \frac{G_{\text{mod.}}}{G_{\text{stat.}}} &= \frac{\sum_{n=0}^{N-1} |a_{0n}|^2}{\sum_{n=0}^{N-1} |A_n|^2} \\ &= \frac{\sum_{n=0}^{N-1} \left| \frac{A_n}{T} [\sin(2\pi C + \phi_n) - \sin \phi_n] \right|^2}{\sum_{n=0}^{N-1} |A_n|^2} \end{aligned} \quad 5-8$$

As indicated in Table III, p. 38, typical gain reductions were found to be about 2 to 4 db., depending upon the parameters selected.

## 6. Model IV

The final form of array modulation to be studied in this investigation consists of a device which periodically shifts between two discrete values the phase of the signal induced in each element. The electronic phase shifters required for this type of system lie within the present state-of-the-art. Each feed line contains a device which shifts the phase of the incoming signal between two values: (1)  $\phi_A$  for the first half of the modulating period, and (2)  $\phi_B$  for the second half. The system is shown schematically in Figure 19, p. 68. The values of  $\phi_A$  and  $\phi_B$  are independent in each of the feed lines. Thus,

$$a_n(t) = A_n e^{j\phi_n(t)} \quad 6-1$$

where

$$\phi_n(t) = \begin{cases} \phi_{An} & \text{for } 0 \leq t \leq T/2 \\ \phi_{Bn} & \text{for } T/2 \leq t \leq T \end{cases} \quad 6-2$$

The modulated excitation function is

$$\begin{aligned} a_{on} &= \frac{A_n}{T} \left[ \int_0^{T/2} e^{j\phi_{An}} dt + \int_{T/2}^T e^{j\phi_{Bn}} dt \right] \\ &= \frac{A_n}{T} \left[ e^{j\phi_{An}} t \Big|_0^{T/2} + e^{j\phi_{Bn}} t \Big|_{T/2}^T \right] \\ &= \frac{A_n}{T} \left[ \frac{T e^{j\phi_{An}}}{2} + T e^{j\phi_{Bn}} - \frac{T e^{j\phi_{Bn}}}{2} \right] \\ &= \frac{A_n}{2} (e^{j\phi_{An}} + e^{j\phi_{Bn}}) \end{aligned}$$

$$\begin{aligned}
 a_{0n} &= \frac{A_n}{2} \left[ (\cos \phi_{An} + \cos \phi_{Bn}) + j(\sin \phi_{An} + \sin \phi_{Bn}) \right] \\
 &= \frac{A_n}{2} \left[ 2 \cos \left( \frac{\phi_{An} + \phi_{Bn}}{2} \right) \cos \left( \frac{\phi_{An} - \phi_{Bn}}{2} \right) \right. \\
 &\quad \left. + j 2 \sin \left( \frac{\phi_{An} + \phi_{Bn}}{2} \right) \cos \left( \frac{\phi_{An} - \phi_{Bn}}{2} \right) \right]
 \end{aligned}$$

$$a_{0n} = A_n \cos \left( \frac{\phi_{An} - \phi_{Bn}}{2} \right) \left[ \cos \left( \frac{\phi_{An} + \phi_{Bn}}{2} \right) + j \sin \left( \frac{\phi_{An} + \phi_{Bn}}{2} \right) \right]$$

6-3

An expression for the filtered signal from the array is

$$v(\theta, \phi, t) = \epsilon(\theta, \phi) e^{j\omega t} \sum_{n=0}^{N-1} A_n e^{jnKd \cos \theta} \cdot$$

$$\cdot \cos \left( \frac{\phi_{An} - \phi_{Bn}}{2} \right) \left[ \cos \left( \frac{\phi_{An} + \phi_{Bn}}{2} \right) + j \sin \left( \frac{\phi_{An} + \phi_{Bn}}{2} \right) \right]$$

6-4

The excitation coefficient at the carrier frequency resulting from this form of modulation is more interesting than those produced by the previous models in that it is a complex function of two variables. This implies that an angle as well as a magnitude is now associated with the multipliers. The normalized carrier frequency coefficient was previously determined to be

$$a_{0n} = \cos \left( \frac{\phi_{An} - \phi_{Bn}}{2} \right) \left[ \cos \left( \frac{\phi_{An} + \phi_{Bn}}{2} \right) + j \sin \left( \frac{\phi_{An} + \phi_{Bn}}{2} \right) \right]$$

6-5



where

$\phi_{An}$  = phase state of the nth element for  $0 \leq t \leq T/2$

$\phi_{Bn}$  = phase state of the nth element for  $T/2 \leq t \leq T$

Two sets of values for  $\phi_{An}$  and  $\phi_{Bn}$  are quite interesting. The first is the case in which  $\phi_{Bn} = -\phi_{An}$  results from a type of flip-flop phase reversal network. The expression for  $a_{on}$  reduces to

$$a_{on} = \cos \phi_{An} (\cos 0 + j \sin 0) = \cos \phi_{An} \quad 6-6$$

Any of the distributions which have been previously discussed can be conveniently obtained by the proper choices of  $\phi_{An}$ . The second set of parameters which have a predictable effect upon the coefficient is  $\phi_{Bn} = \phi_{An} \pm 180^\circ$ . This unwise choice will result in a value of  $a_{on}$  equal to zero, since

$$\begin{aligned} a_{on} &\propto \cos \left( \frac{\phi_{An} - \phi_{Bn}}{2} \right) \\ &\propto \cos \left( \frac{\phi_{An} - \phi_{An} \mp 180^\circ}{2} \right) \\ &\propto \cos (\mp 90^\circ) \equiv 0 \end{aligned} \quad 6-7$$

With this coefficient equal to zero, there will be no signal from the array at the carrier frequency.

All other combinations of  $\phi_{An}$  and  $\phi_{Bn}$  will, in general, result in a complex expression for the unmodulated excitation coefficient of the form

$$a_{on} = \delta_n \angle \gamma_n \quad 6-8$$

where

$\delta_n$  = the magnitude of the modulation signal in the nth element

$\gamma_n$  = the phase angle of the modulation signal in the nth element

A nomogram was prepared to aid in the computation of  $\delta_n$  and  $\gamma_n$  from given values of  $\phi_{An}$  and  $\phi_{Bn}$ , and visa versa. This is shown in Figure 20, p. 68, for  $0 \leq \delta_n \leq 1$  and  $-90^\circ \leq \gamma_n \leq 90^\circ$ . To determine the values of  $\delta$  and  $\gamma$ , the abscissa and ordinate are entered with the given values of  $\phi_A$  and  $\phi_B$ . The diagonal lines which pass through the resulting point indicate the magnitude and phase angle of the particular multiplier. For example, if  $\phi_A = 60^\circ$  and  $\phi_B = 20^\circ$ , the value of  $\delta/\gamma$  would be  $0.766/20^\circ$ . To determine the values of  $\phi_A$  and  $\phi_B$  which will produce a desired  $\delta/\gamma$ , the nomogram may be entered in either of two places with  $\delta$  and  $\gamma$ ; two sets of  $\phi_A$  and  $\phi_B$  values will result. As an example, if it is desired to realize a multiplier equal to  $0.5/15^\circ$ , either of the two sets ( $\phi_A = 75^\circ$ ,  $\phi_B = -45^\circ$ ) or ( $\phi_A = -45^\circ$ ,  $\phi_B = 75^\circ$ ) may be employed. This form of modulation gives the designer a much wider latitude in the determination of element multipliers than was possible in the previous forms discussed. Any distribution for the magnitude and phase of the element excitations can be realized by the proper choice of modulation parameters.

A number of field patterns were calculated for various magnitude distributions of the modulated excitation coefficient,  $\delta_n$ , with the phase angle,  $\gamma_n$ , equal to zero. The results were in good agreement with those expected from the theory; array patterns were produced with a significant reduction in the magnitude of the sidelobes. Table IV presents a summary of the calculated values.

In an effort to possibly reduce the beam width or to achieve a beam steering capability without resorting to phase delays in the feed lines, distributions of  $\delta_n$  were tested with  $\gamma_n$  free to vary from  $-90$  to  $+90$  degrees. The results of this phase of the investigation were disappoint-

TABLE IV

## CALCULATED FIELD PATTERNS FOR MODEL IV

Type of Modulation	$\phi_{A1}$ , $\phi_{A8}$ (deg.)	$\phi_{B1}$ , $\phi_{B8}$ (deg.)	$\phi_{A2}$ , $\phi_{A7}$ (deg.)	$\phi_{B2}$ , $\phi_{B7}$ (deg.)	$\phi_{A3}$ , $\phi_{A6}$ (deg.)	$\phi_{B3}$ , $\phi_{B6}$ (deg.)	$\phi_{A4}$ , $\phi_{A5}$ (deg.)	$\phi_{B4}$ , $\phi_{B5}$ (deg.)	Beam Width (deg.)	1st Side-lobe (db.)	2nd Side-lobe (db.)	3rd Side-lobe (db.)	Gain w/r/t Static (db.)
Static	0.0	0.0	0.0	0.0	0.0	0.0	0.0	0.0	17.5	-12.8	-16.4	-17.9	0.0
180 Reversal	75.0	225.0	50.0	230.0	25.0	205.0	0.0	180.0	Zero output for all values of $\theta$ .				
Misc.	60.0	0.0	40.0	0.0	20.0	0.0	0.0	0.0	18.2	-15.5	-15.5	-18.2	-0.45
Misc.	30.0	0.0	20.0	0.0	10.0	0.0	0.0	0.0	17.8	-17.0	-15.7	-18.0	-0.12
Misc.	83.0	-64.5	68.0	-49.5	44.5	-25.5	10.0	10.0	23.7	-30.6	-32.4	-29.0	-2.97
30 db. Dolph-Tcheby.	74.4	-74.4	58.1	-58.1	34.9	-34.9	0.0	0.0	22.6	-29.0	-30.1	-29.8	-2.96
40 db. Dolph-Tcheby.	81.7	-81.7	65.6	-65.6	40.9	-40.9	0.0	0.0	24.2	-41.7	-39.9	-39.9	-3.56

ing. A slight degree of beam steering was achieved, but in an unpredictable manner. The beam width did decrease in some cases; however, it was accompanied by new and much stronger sidelobes. While successful joint distributions of  $\delta_n$  and  $\gamma_n$  which would accomplish more than side-lobe reduction were not uncovered, the additional degree of freedom seems to indicate that they would exist. A search for distributions which would achieve some of these desired properties might present a basis for further research in this area.

This particular type of modulation is similar to all other forms in that part of the received signal is converted into the sideband spectrum about the carrier frequency. In order to determine the extent to which this sideband signal detracts from the desired signal, it is necessary to obtain a generalized expression for the modulated excitation coefficient,  $a_{mn}$ . From equation 2-6,

$$a_{mn} = \frac{1}{T} \int_0^T a_n(t) e^{-j\omega_m t} dt \quad 6-9$$

where

$$a_n(t) = A_n e^{j\phi_n(t)}$$

and

$$\phi_n(t) = \begin{cases} \phi_{An} & \text{for } 0 \leq t \leq T/2 \\ \phi_{Bn} & \text{for } T/2 \leq t \leq T \end{cases}$$



Therefore,

$$\begin{aligned}
 a_{mn} &= \frac{A_n}{T} \left[ \int_0^{T/2} e^{j\phi_{An}} e^{-j\omega_m t} dt + \int_{T/2}^T e^{j\phi_{Bn}} e^{-j\omega_m t} dt \right] \\
 &= \frac{A_n}{T} \left[ e^{j\phi_{An}} \frac{e^{-j\omega_m t}}{-j\omega_m} \Big|_0^{T/2} + e^{j\phi_{Bn}} \frac{e^{-j\omega_m t}}{-j\omega_m} \Big|_{T/2}^T \right] \\
 &= \frac{A_n}{T} \left[ \frac{e^{j\phi_{An}}}{-j\omega_m} (e^{-j\frac{\omega_m T}{2}} - 1) + \frac{e^{j\phi_{Bn}}}{-j\omega_m} (e^{-j\omega_m T} - e^{-j\frac{\omega_m T}{2}}) \right] \\
 &= \frac{A_n}{-j\omega_m T} \left[ e^{j\phi_{An}} (e^{-j\frac{\omega_m T}{2}} - 1) + e^{j\phi_{Bn}} e^{-j\frac{\omega_m T}{2}} (e^{-j\frac{\omega_m T}{2}} - 1) \right] \\
 &= \frac{A_n}{-j\omega_m T} \left[ (e^{j\phi_{An}} + e^{j(\phi_{Bn} - \frac{\omega_m T}{2})}) (e^{-j\frac{\omega_m T}{4}} e^{-j\frac{\omega_m T}{4}} - e^{-j\frac{\omega_m T}{4}} e^{j\frac{\omega_m T}{4}}) \right] \\
 &= \frac{2A_n}{\omega_m T} \left[ (e^{j\phi_{An}} + e^{j(\phi_{Bn} - \frac{\omega_m T}{2})}) e^{-j\frac{\omega_m T}{4}} \left( \frac{e^{j\frac{\omega_m T}{4}} - e^{-j\frac{\omega_m T}{4}}}{2j} \right) \right] \\
 &= \frac{2A_n}{\omega_m T} \left[ (e^{j\phi_{An}} + e^{j(\phi_{Bn} - \frac{\omega_m T}{2})}) (\sin \frac{\omega_m T}{4}) e^{-j\frac{\omega_m T}{4}} \right] \\
 &= \frac{2A_n}{\omega_m T} \left\{ [e^{j\phi_{An}} + e^{j(\phi_{Bn} - \frac{\omega_m T}{2})}] (\sin \frac{\omega_m T}{4}) (\cos \frac{\omega_m T}{4} - j \sin \frac{\omega_m T}{4}) \right\} \\
 a_{mn} &= \frac{A_n}{\omega_m T} \left[ e^{j\phi_{An}} + e^{j(\phi_{Bn} - \frac{\omega_m T}{2})} \right] \left[ \sin \frac{\omega_m T}{2} - j(1 - \cos \frac{\omega_m T}{2}) \right]
 \end{aligned}$$

6-10



However, since

$$\omega_m T = m\omega_0 T = 2\pi m ; m = \pm 1, \pm 2, \dots, \pm M \quad 6-11$$

the following relationships exist:

$$\sin \frac{\omega_m T}{2} = \sin \pi m \equiv 0 \quad 6-12$$

$$\cos \frac{\omega_m T}{2} = \cos \pi m = (-1)^m \quad 6-13$$

and

$$(1 - \cos \frac{\omega_m T}{2}) = 1 - (-1)^m = \begin{cases} 0 & \text{for } m \text{ even} \\ +2 & \text{for } m \text{ odd} \end{cases} \quad 6-14$$

As a result, there will only be odd-numbered sideband frequencies in the output signal of the array.

$$a_{mn} = \frac{A_n}{2\pi m} [e^{j\phi_{An}} + e^{j(\phi_{Bn} - m\pi)}] (-j2) ; m \text{ odd}$$

$$= \frac{-jA_n}{m\pi} \left\{ [\cos \phi_{An} + \cos (\phi_{Bn} - m\pi)] \right.$$

$$\left. + j [\sin \phi_{An} + \sin (\phi_{Bn} - m\pi)] \right\}$$

$$a_{mn} = \frac{-j2A_n}{m\pi} \left[ \left( \cos \frac{\phi_{An} + \phi_{Bn} - m\pi}{2} \cos \frac{\phi_{An} - \phi_{Bn} + m\pi}{2} \right) \right.$$

$$\left. + j \left( \sin \frac{\phi_{An} + \phi_{Bn} - m\pi}{2} \cos \frac{\phi_{An} - \phi_{Bn} + m\pi}{2} \right) \right]$$

$$\operatorname{Re}[a_{mn}] = \frac{2A_n}{m\pi} \left( \sin \frac{\phi_{An} + \phi_{Bn} - m\pi}{2} \cos \frac{\phi_{An} - \phi_{Bn} + m\pi}{2} \right) ; m \text{ odd}$$

$$\operatorname{Im}[a_{mn}] = -\frac{2A_n}{m\pi} \left( \cos \frac{\phi_{An} + \phi_{Bn} - m\pi}{2} \cos \frac{\phi_{An} - \phi_{Bn} + m\pi}{2} \right) ; m \text{ odd}$$

Therefore,

$$a_{mn} = \frac{2A_n}{m\pi} \cos \frac{\phi_{An} - \phi_{Bn} + m\pi}{2} \left( \sin \frac{\phi_{An} + \phi_{Bn} - m\pi}{2} - j \cos \frac{\phi_{An} + \phi_{Bn} - m\pi}{2} \right)$$

for  $m$  odd 6-15

and

$$a_{mn} = 0 \quad \text{for } m \text{ even} \quad \text{6-16}$$

From equation 6-5, for  $m = 0$ :

$$a_{0n} = A_n \cos \frac{\phi_{An} - \phi_{Bn}}{2} \left( \cos \frac{\phi_{An} + \phi_{Bn}}{2} + j \sin \frac{\phi_{An} + \phi_{Bn}}{2} \right)$$

The sideband signal developed by the modulated array is then equal to

$$v_{s,b}(\theta, \phi, t) = \epsilon(\theta, \phi) \sum_{m \text{ odd}} e^{j(\omega + m\omega_0)t} \sum_{n=0}^{N-1} a_{mn} e^{jnKd \cos \theta}$$

6-17

Figure 21, p. 69, shows the signal levels at the carrier and the first and third sideband frequencies for a desired sidelobe reduction of 40 db. The results clearly show the necessity for employing a narrow band pass filter centered about the carrier frequency. Both of the

sideband signals are considerably stronger than the desired signal for angles of more than about  $20^\circ$  from the boresight axis. These frequencies must be filtered out prior to detection in order to achieve the -40 db. sidelobes.

## 7. Conclusions

This investigation has demonstrated the ability of parameter modulation to reduce the sidelobe level of a linear antenna array. The modulation can take practically any form, and can be used to vary such factors as the apparent length of the array and the phase and frequency relationships in the various feed lines. The signal from the array must be filtered prior to detection as it contains additional sideband signals generated by the modulation process. In accordance with the sampling theorem, the modulating frequency must be greater than twice the highest frequency component contained in the information-carrying signal.

Four specific types of modulation were investigated in this study.

They were:

1. Model I with parameter  $\tau_n$ , the ON time of the nth element.
2. Model II with parameter  $b_n$ , the frequency controlling factor in the nth feed line.
3. Model III with the parameters  $C$ , a frequency factor common to all feed lines, and  $\phi_n$ , the relative phase in the nth feed line.
4. Model IV with parameters  $\phi_{An}$  and  $\phi_{Bn}$ , the relative phases in the nth feed line during the first-half and the second-half periods of modulation.

The radiation patterns formed by varying the parameter distributions in each of the four models were compared to the static, or unmodulated, array pattern. It was found that:

1. The sidelobe level was reduced by more than an order of magnitude with the proper parameter selection.
2. The loss in receiving antenna gain caused by the modulation was generally from 2 to 4 db.

3. The beam width of the receiving pattern increased as the sidelobe level was reduced.
4. The main beam could be steered through an arc of about  $70^\circ$ , while the modulation held the sidelobe level to the desired value.
5. In order to realize the intended sidelobe reduction and preserve the information content of the signal, strict requirements must be placed upon the band-pass filter prior to detection.

There are a number of specific topics which require further study in this area. For example:

1. How can modulation be applied to other types of antenna systems?
2. What desirable properties other than sidelobe reduction can be realized by antenna modulation?
3. How does the modulation affect the mutual coupling between the individual elements?
4. What other types of modulation could be applied to an array?
5. Referring to Model IV in this study, what joint distributions of  $\delta_n$  and  $\mathcal{V}_n$  could be used in order to achieve beam steering or a reduced beam width?

The use of time as a design parameter does give an additional degree of freedom to the linear receiving array. How effective this technique will become depends, in part, upon the answers to the above questions. Modulation is a relatively new concept in antenna design. Its full potential has yet to be developed; however, the philosophy of time modulated antennas does warrant further study.



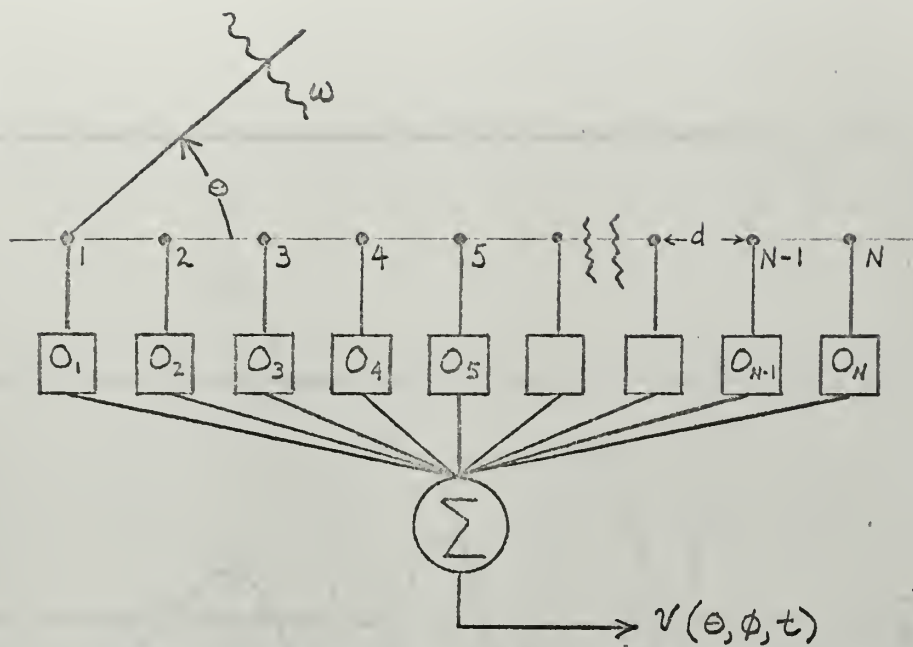


Figure 1. Linear antenna array used in this study.

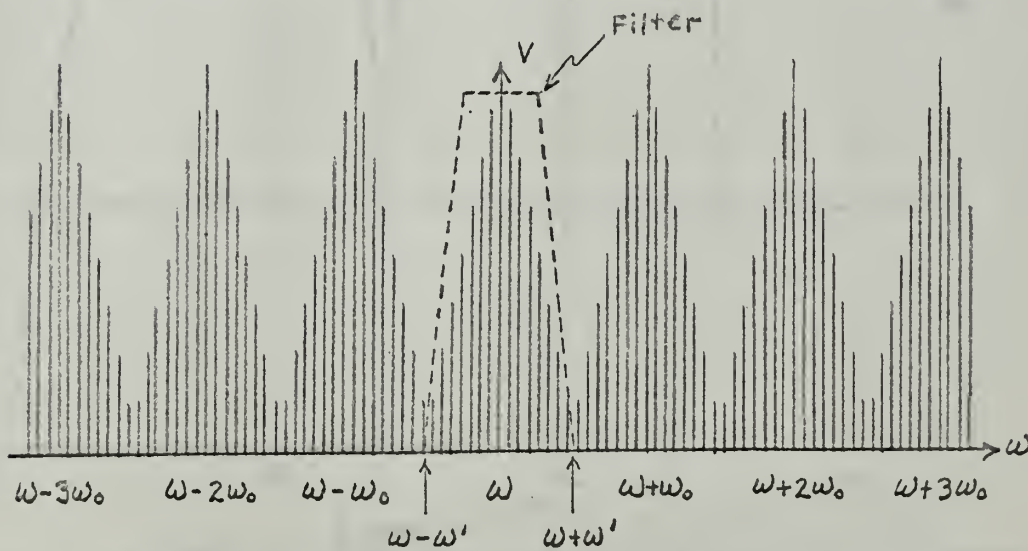


Figure 2. Frequency spectrum of the signal from the modulated array,  $v(\theta, \phi, t)$ .

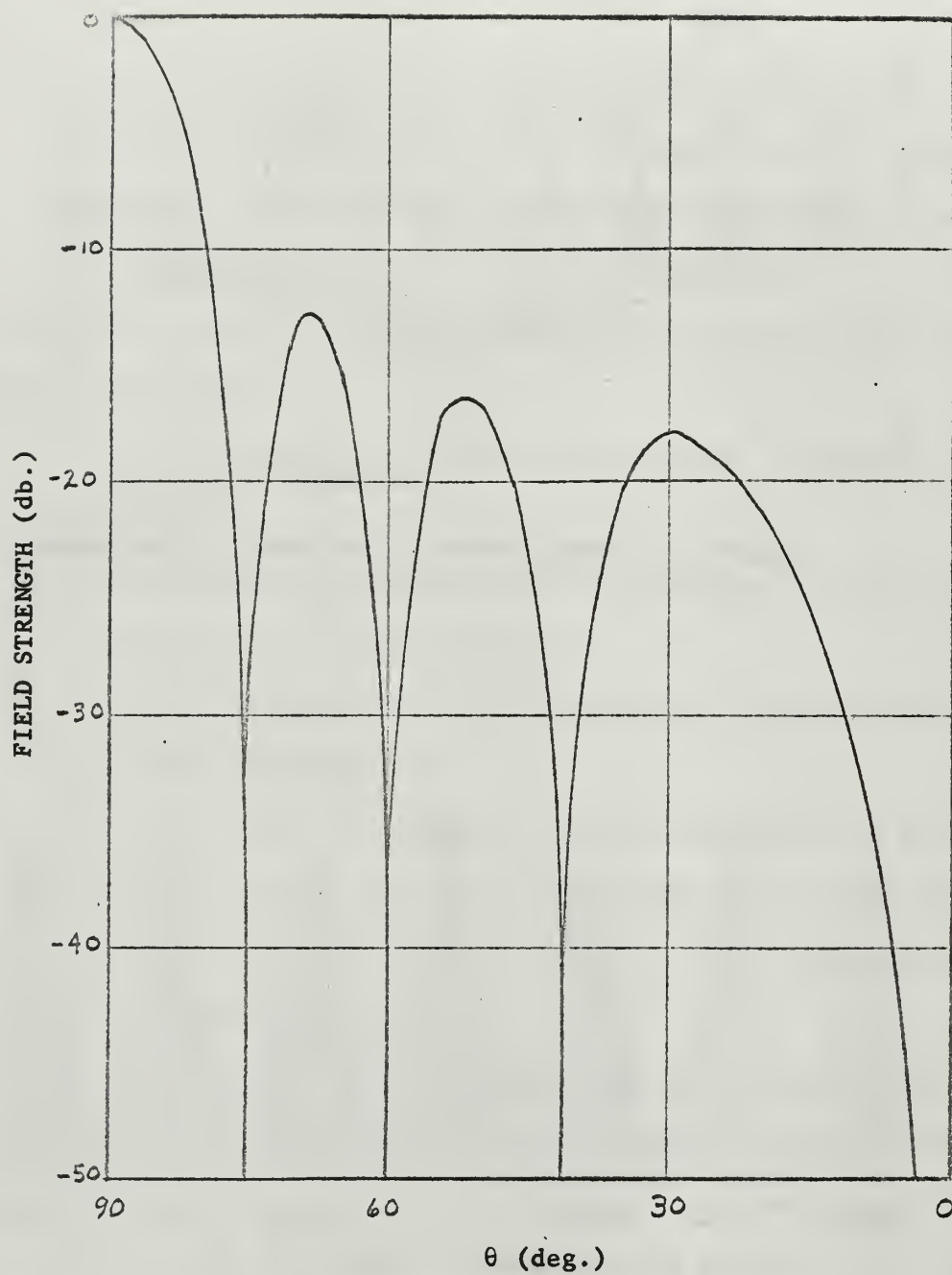


Figure 3. Static, or unmodulated, array field pattern for Model I with  $\gamma_1 = \gamma_2 = \dots = \gamma_8 = 1.0$

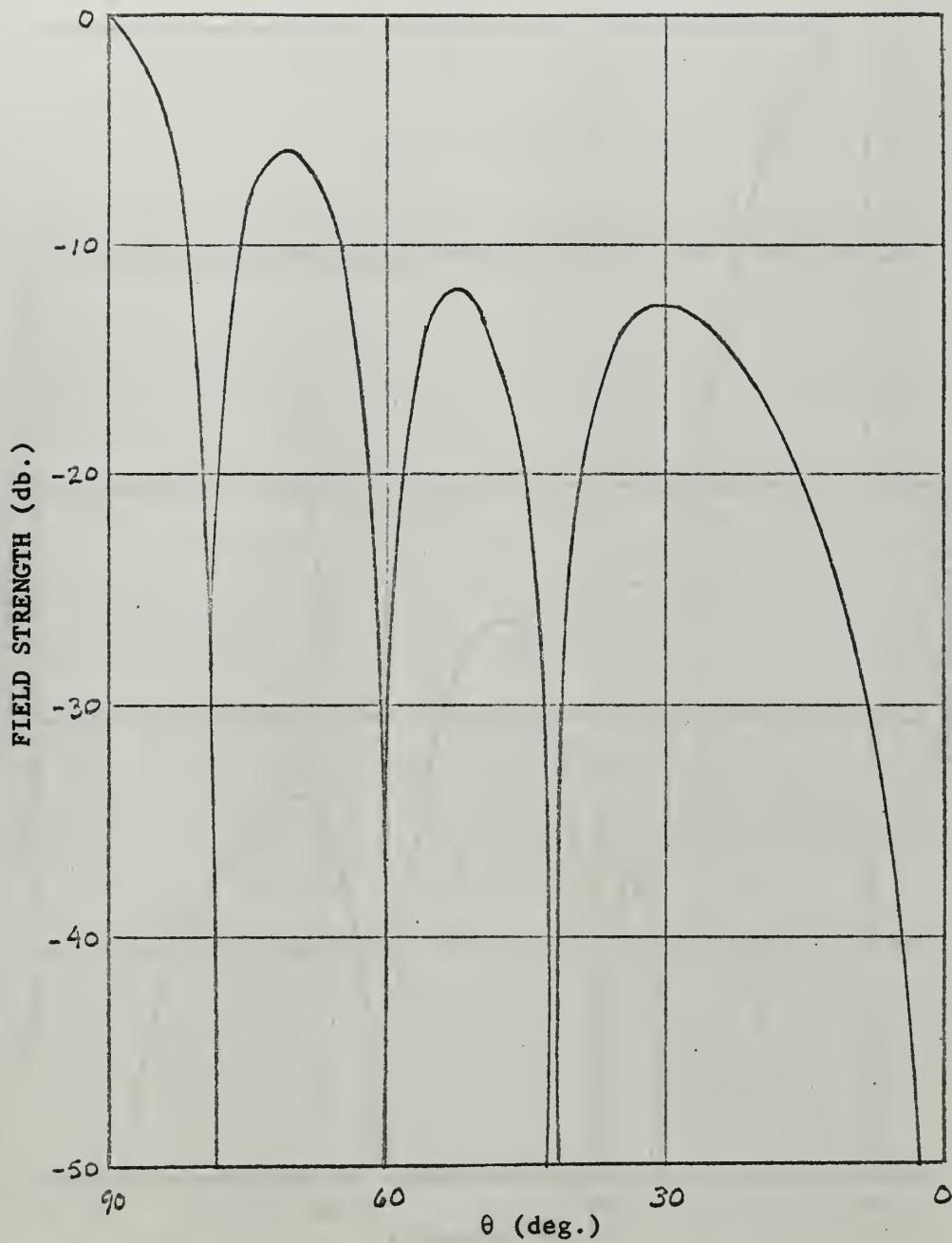


Figure 4. Array field pattern for Model I with inversely and linearly tapered ON times:  $\tau_1 = \tau_8 = 1.0$ ,  $\tau_2 = \tau_7 = 0.75$ ,  $\tau_3 = \tau_6 = 0.50$ , and  $\tau_4 = \tau_5 = 0.25$ .

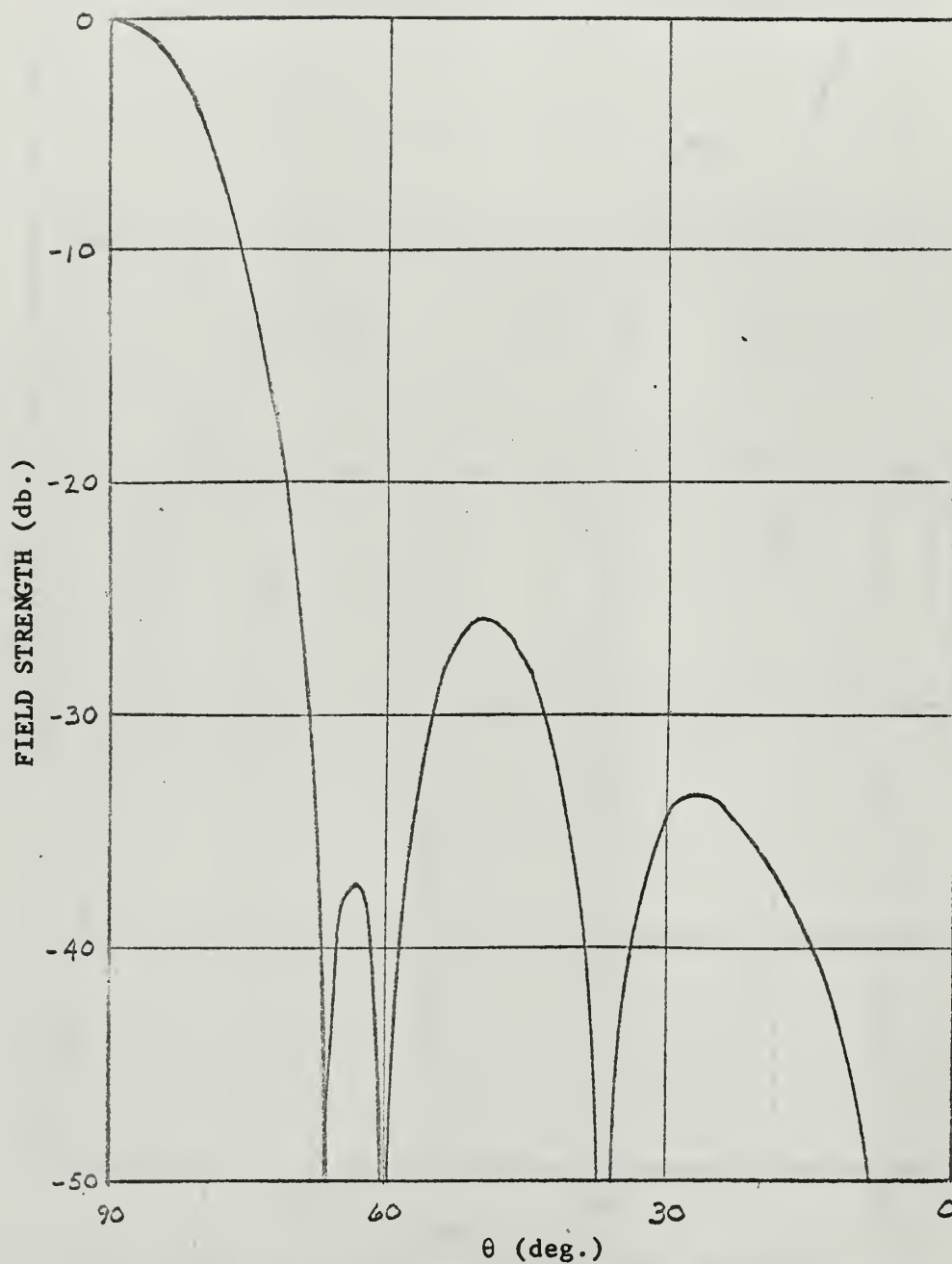


Figure 5. Array field pattern for Model I with linearly tapered ON times:  $\tau_1 = \tau_8 = 0.25$ ,  $\tau_2 = \tau_7 = 0.50$ ,  $\tau_3 = \tau_6 = 0.75$ , and  $\tau_4 = \tau_5 = 1.0$

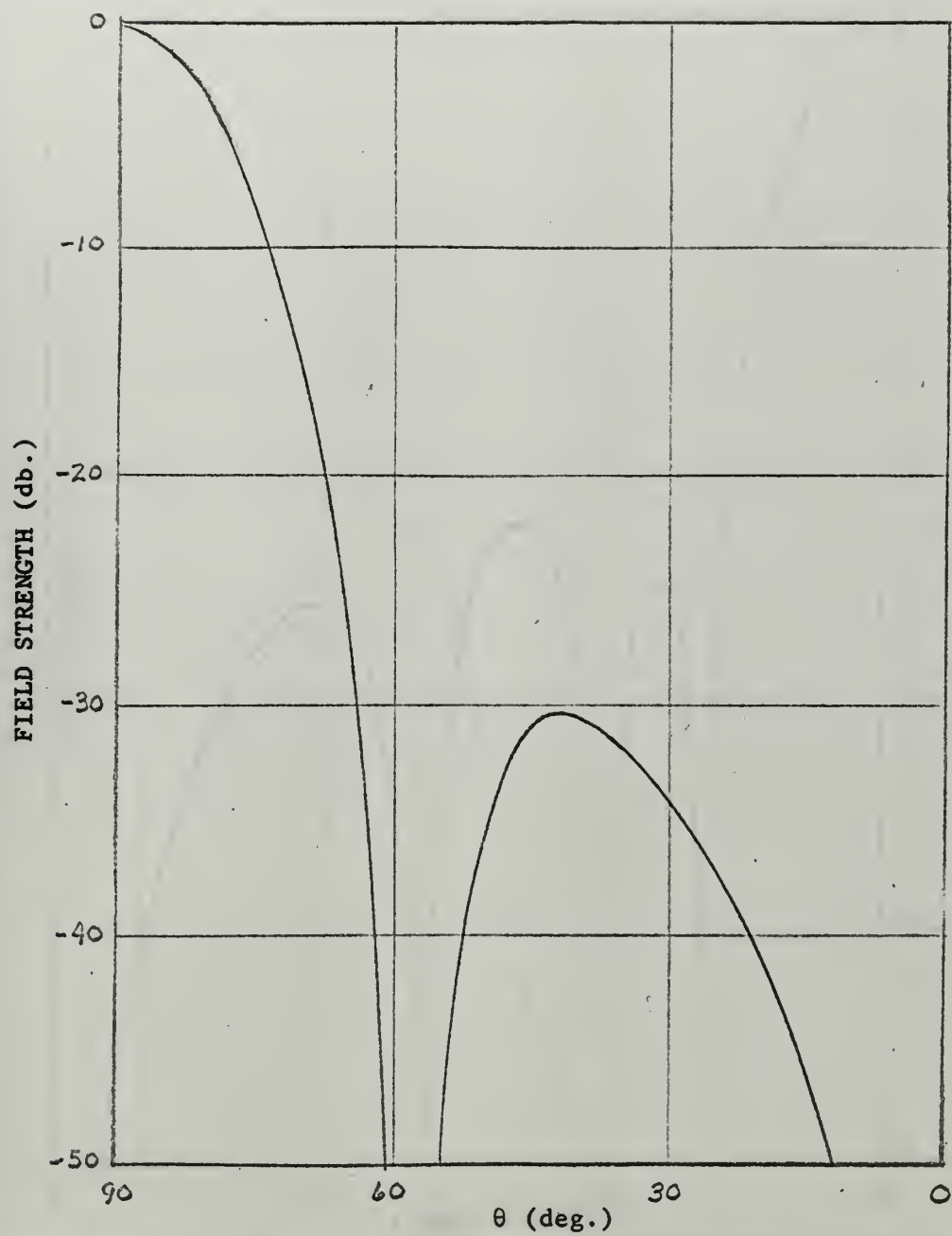


Figure 6. Array field pattern for Model I with linearly tapered ON times:  $\tau_1 = \tau_8 = 0.1$ ,  $\tau_2 = \tau_7 = 0.4$ ,  $\tau_3 = \tau_6 = 0.7$ , and  $\tau_4 = \tau_5 = 1.0$



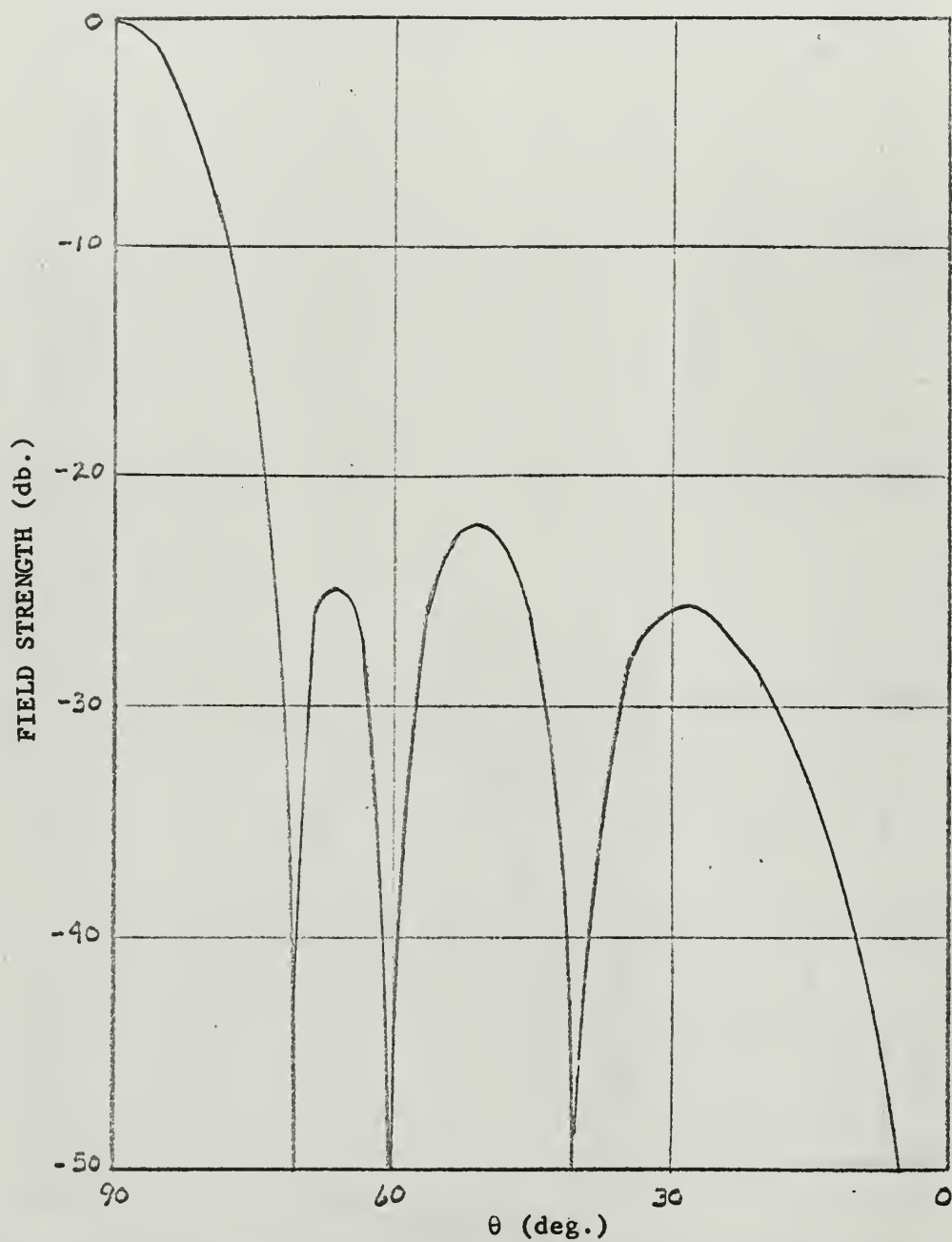


Figure 7. Array field pattern for Model I with linearly tapered ON times:  $\tau_1 = \tau_8 = 0.4$ ,  $\tau_2 = \tau_7 = 0.4$ ,  
 $\tau_3 = \tau_6 = 0.8$ , and  $\tau_4 = \tau_5 = 1.0$

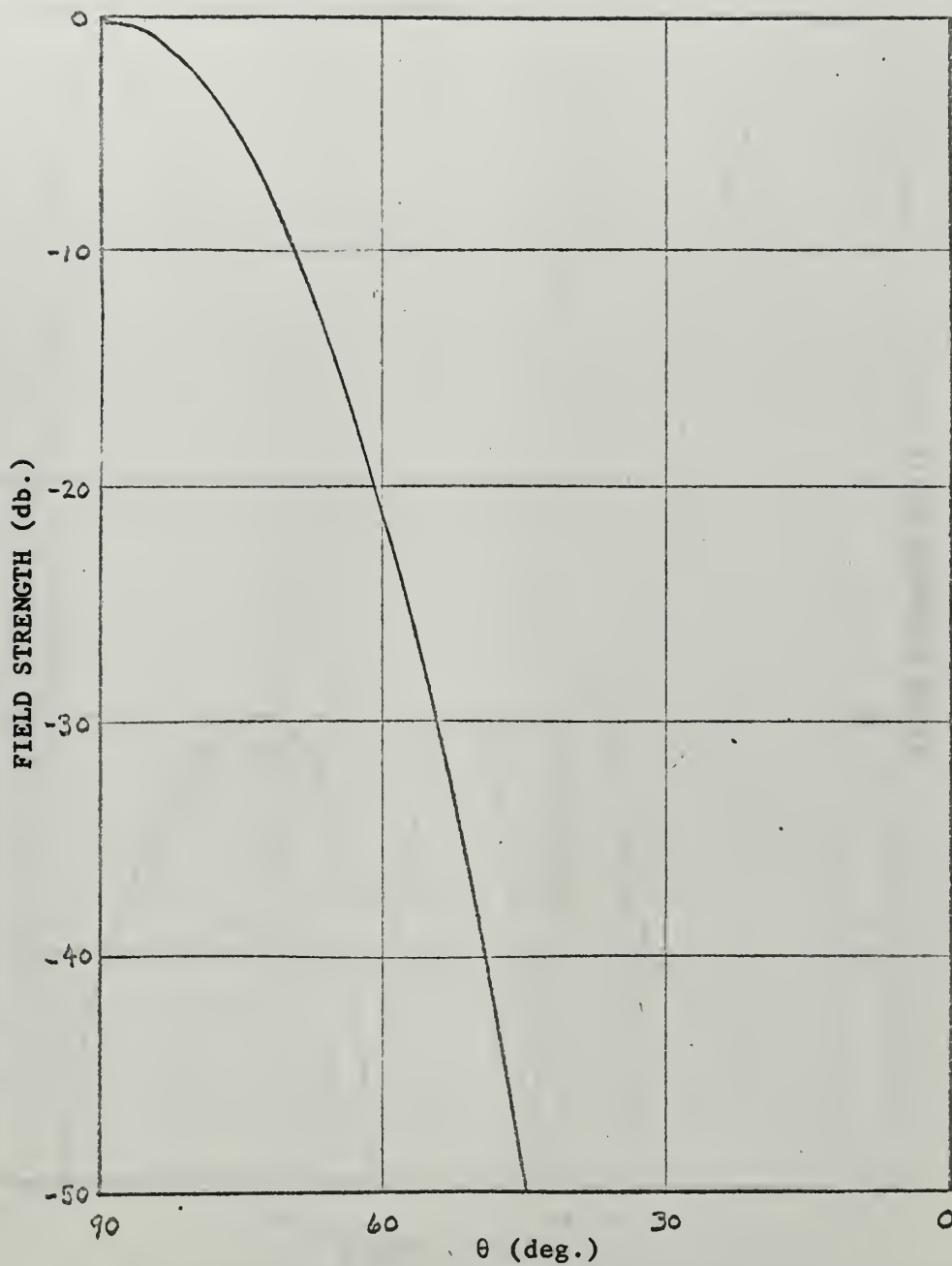


Figure 8. Array field pattern for Model I with a binomial distribution of ON times:  $\tau_1 = \tau_8 = 0.029$ ,  $\tau_2 = \tau_7 = 0.20$ ,  $\tau_3 = \tau_6 = 0.60$ , and  $\tau_4 = \tau_5 = 1.0$

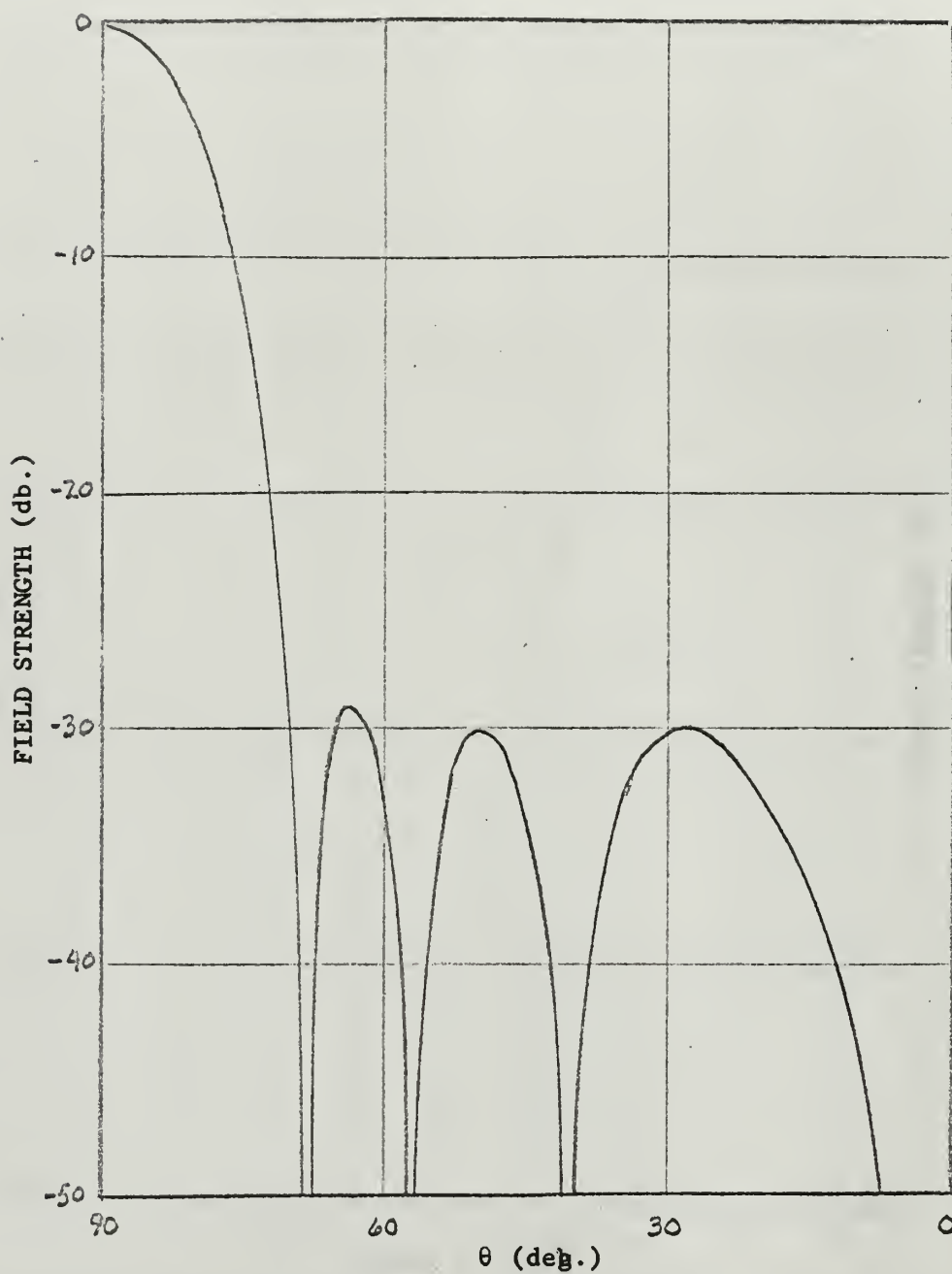


Figure 9. Array field pattern for Model I with a 30 db. Dolph-Tchebyscheff distribution of ON times:

$$\tau_1 = \tau_8 = 0.268, \quad \tau_2 = \tau_7 = 0.528, \quad \tau_3 = \tau_6 = 0.819, \quad \text{and} \\ \tau_4 = \tau_5 = 1.0$$

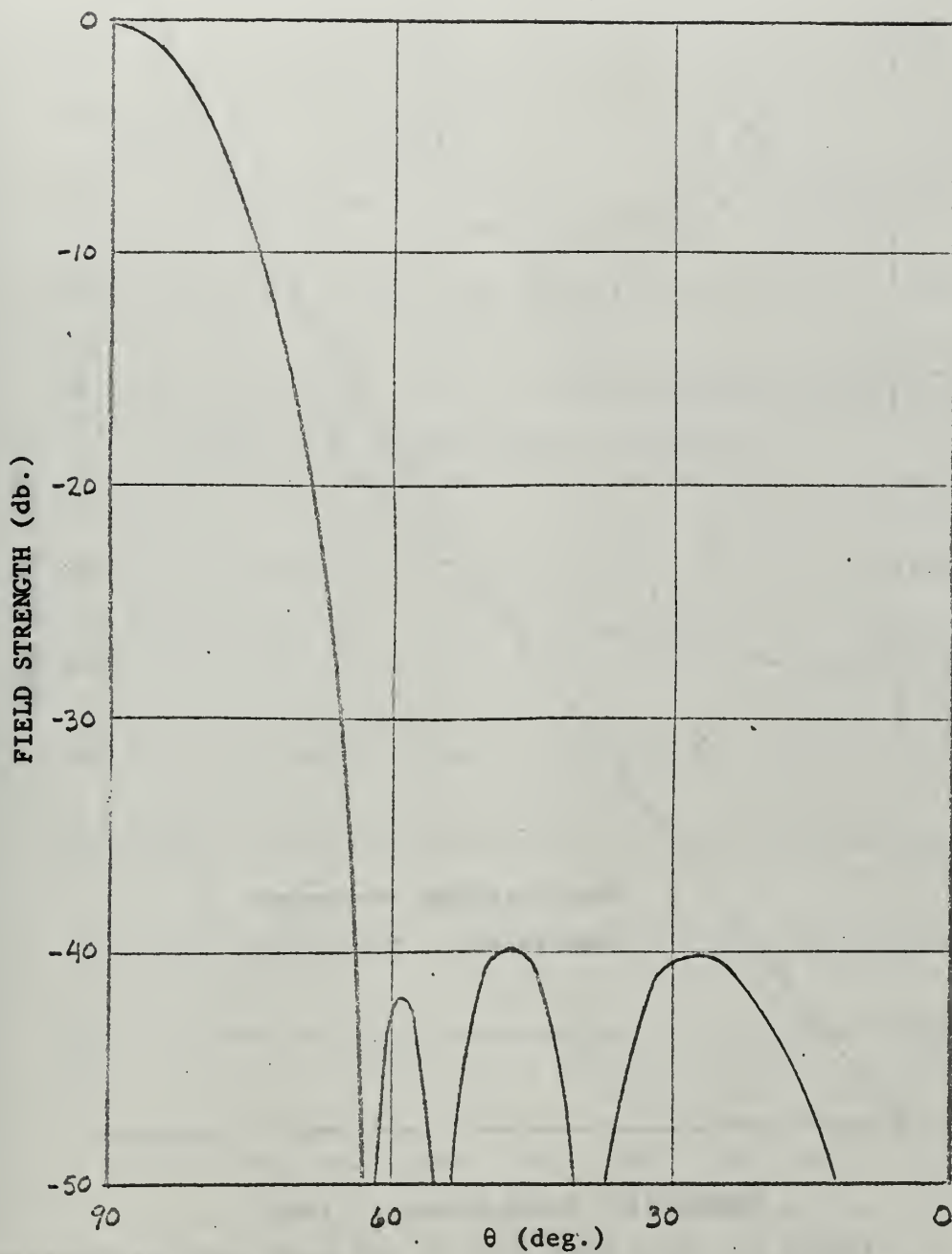


Figure 10. Array field pattern for Model I with a 40 db. Dolph-Tchebyscheff distribution of ON times:  $\tau_1 = \tau_8 = 0.144$ ,  $\tau_2 = \tau_7 = 0.413$ ,  $\tau_3 = \tau_6 = 0.755$ , and  $\tau_4 = \tau_5 = 1.0$

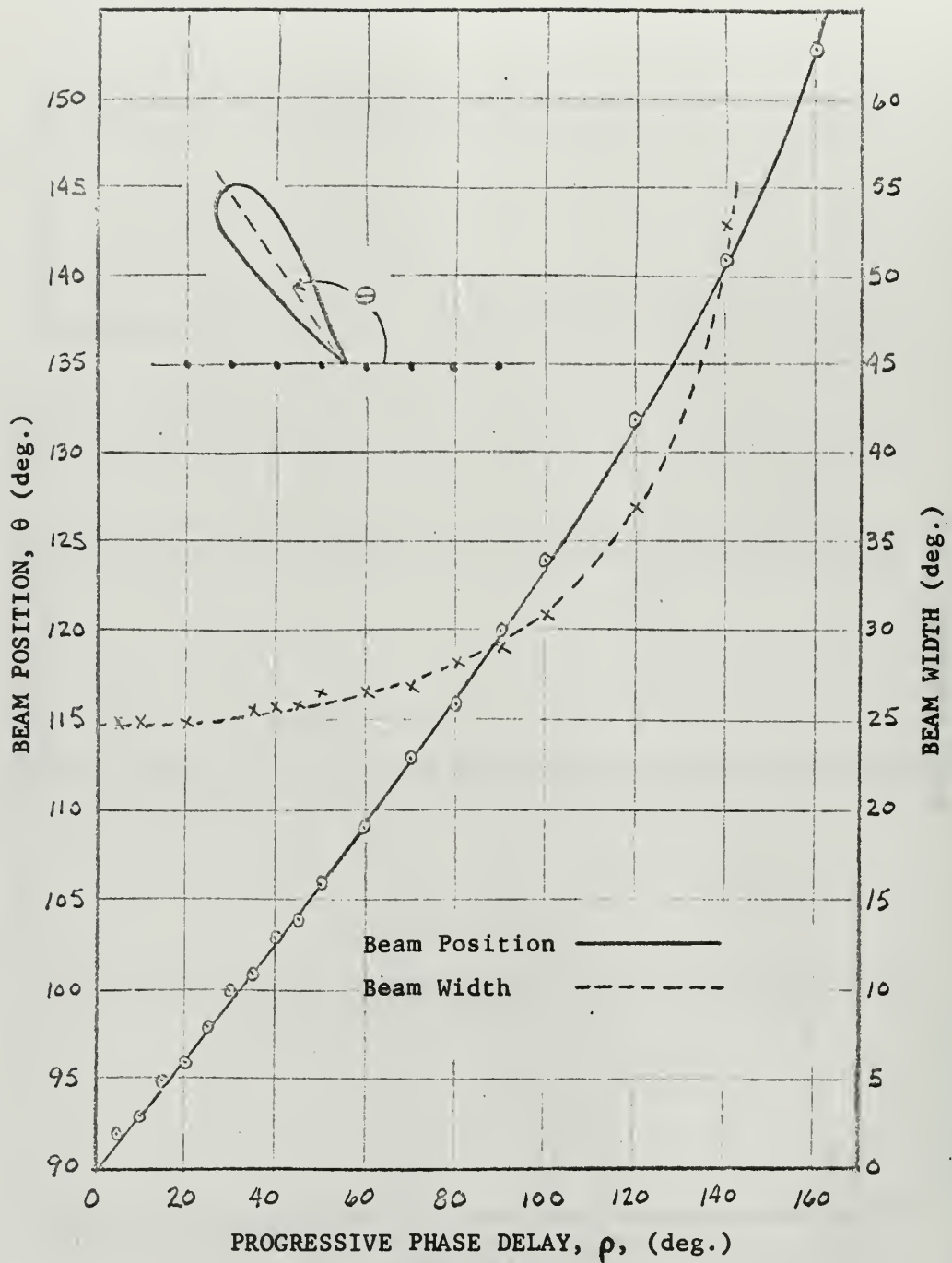


Figure 11. Main beam position and beam width as functions of the progressive element phase delay factor,  $\rho$ .



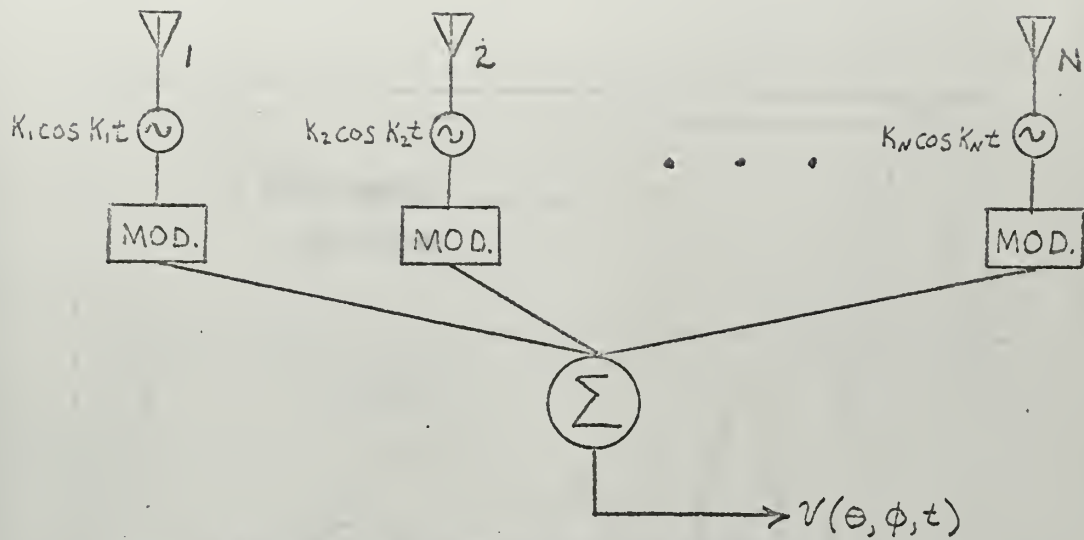


Figure 12. Antenna array for Model II.

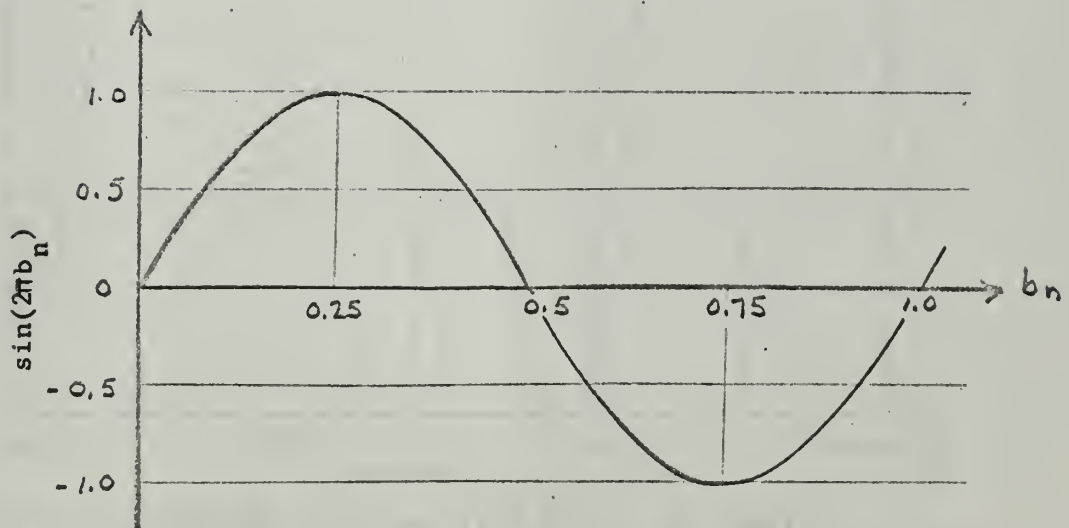


Figure 13.  $\sin(2\pi b_n)$  as a function of  $b_n$ .

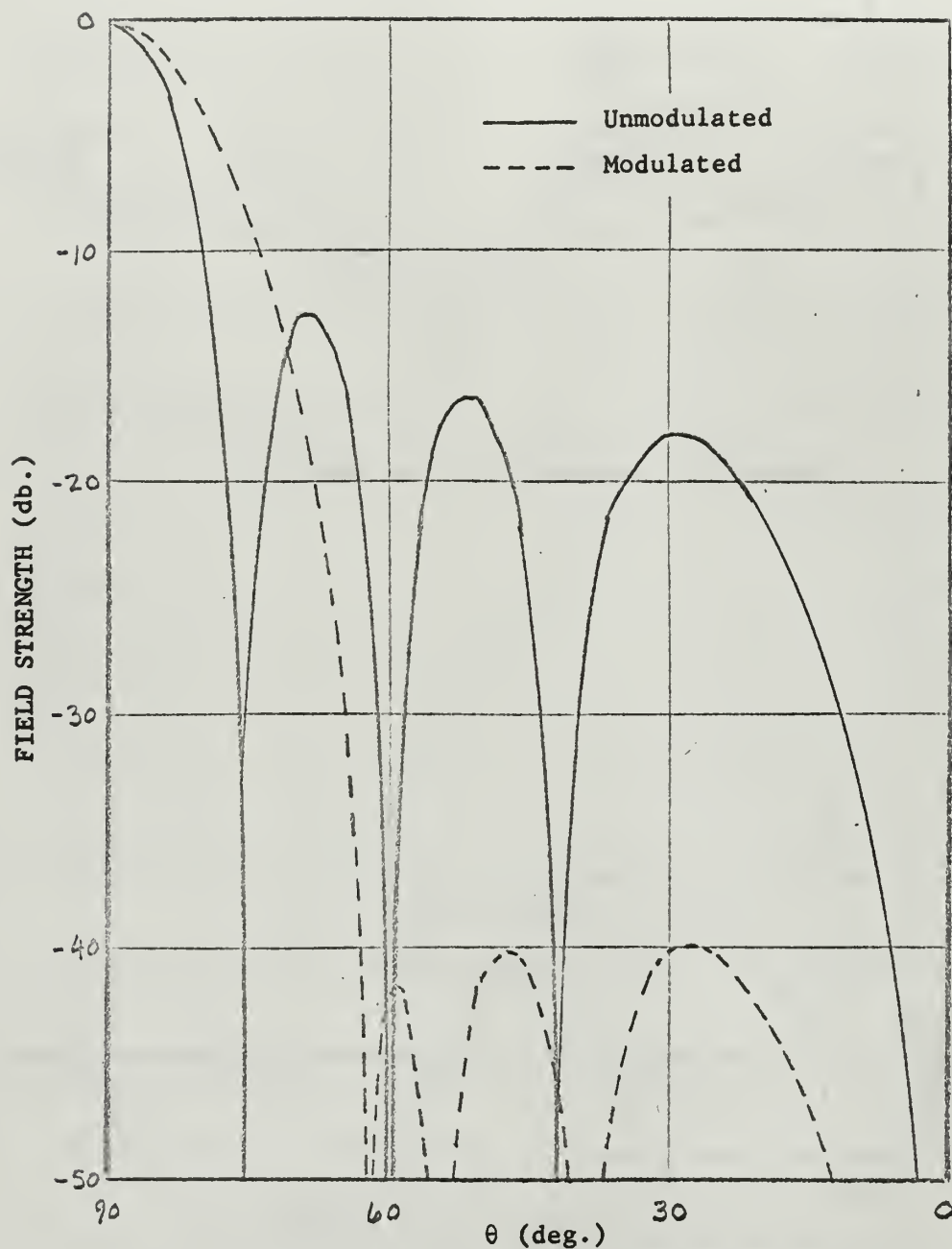


Figure 14. Array field patterns for Model II with no modulation:  $b_1 = b_2 = \dots = b_8 = 0.25$ ; and with a 40 db. Dolph-Tchebyscheff distribution of  $\sin(2\pi b_n)$ :  $b_1 = b_8 = 0.02305$ ,  $b_2 = b_7 = 0.0678$ ,  $b_3 = b_6 = 0.1365$ , and  $b_4 = b_5 = 0.25$ .

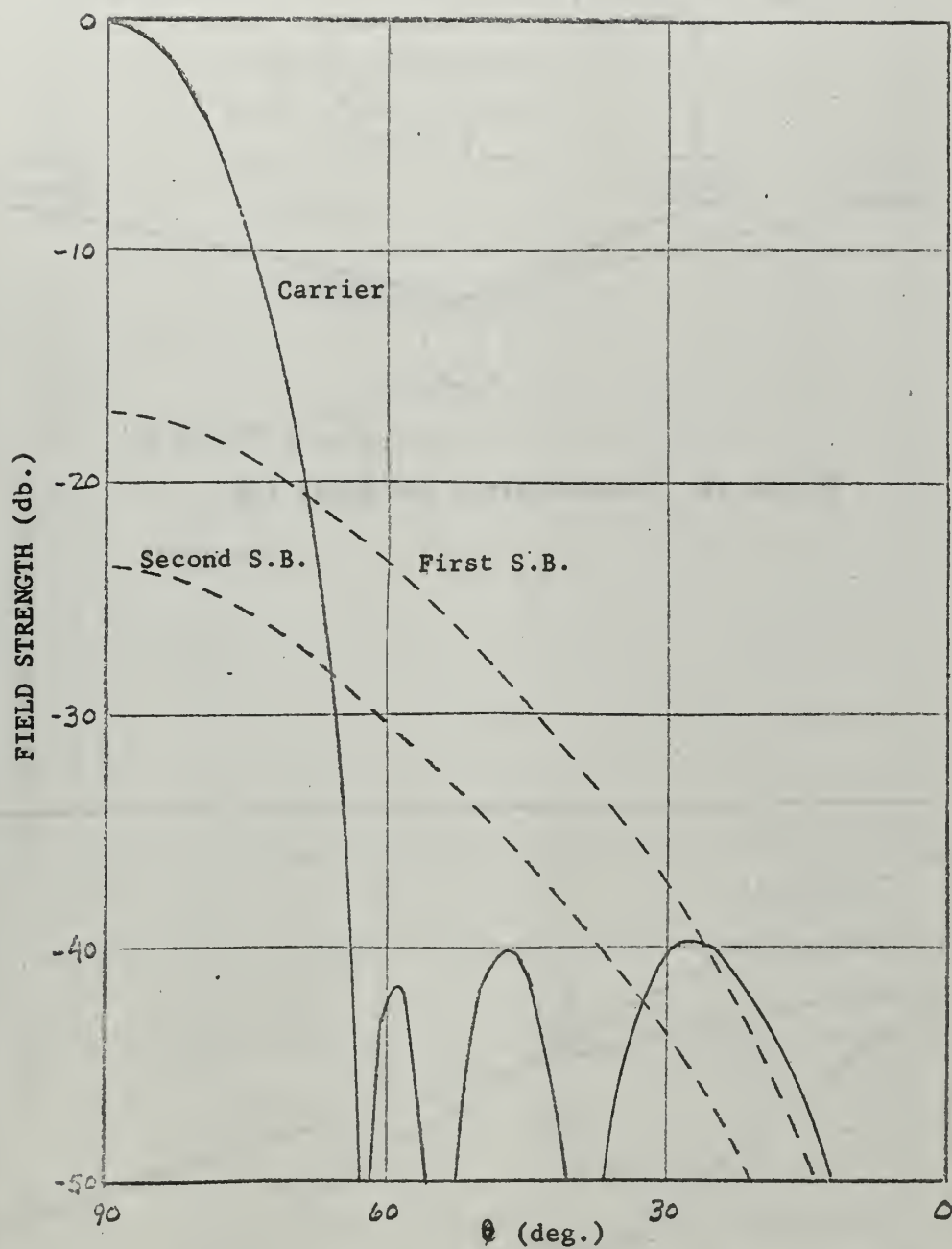


Figure 15. Array field patterns at the carrier and first two sideband frequencies for Model II with a 40 db. Dolph-Tchebyscheff distribution of  $\sin(2\pi b_n)$ .

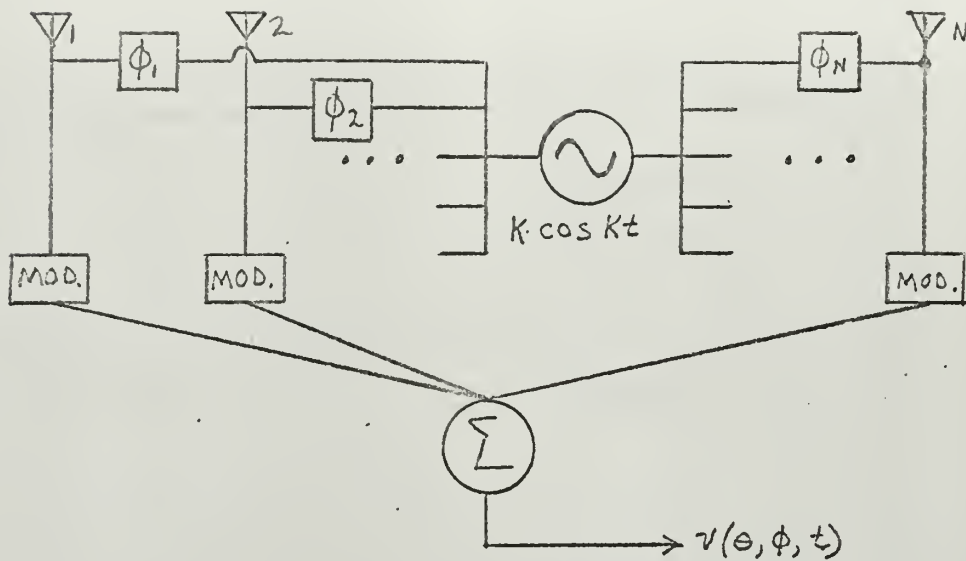


Figure 16. Antenna array for Model III.

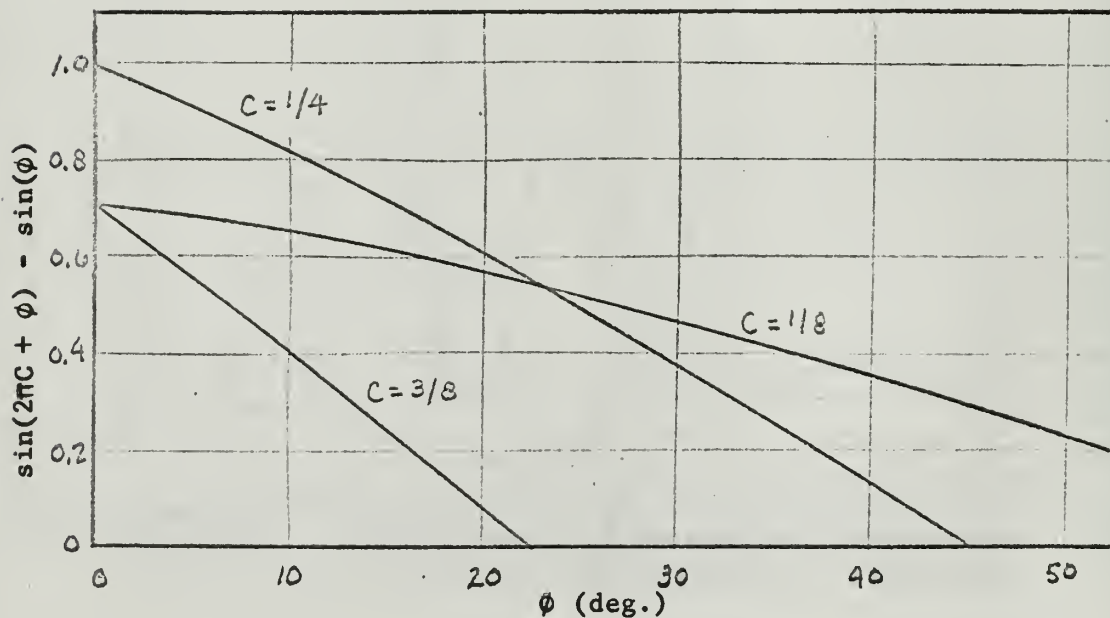


Figure 17.  $[\sin(2\pi C + \phi) - \sin \phi]$  as a function of  $\phi$  for  $C = 1/8, 1/4$ , and  $3/8$ .

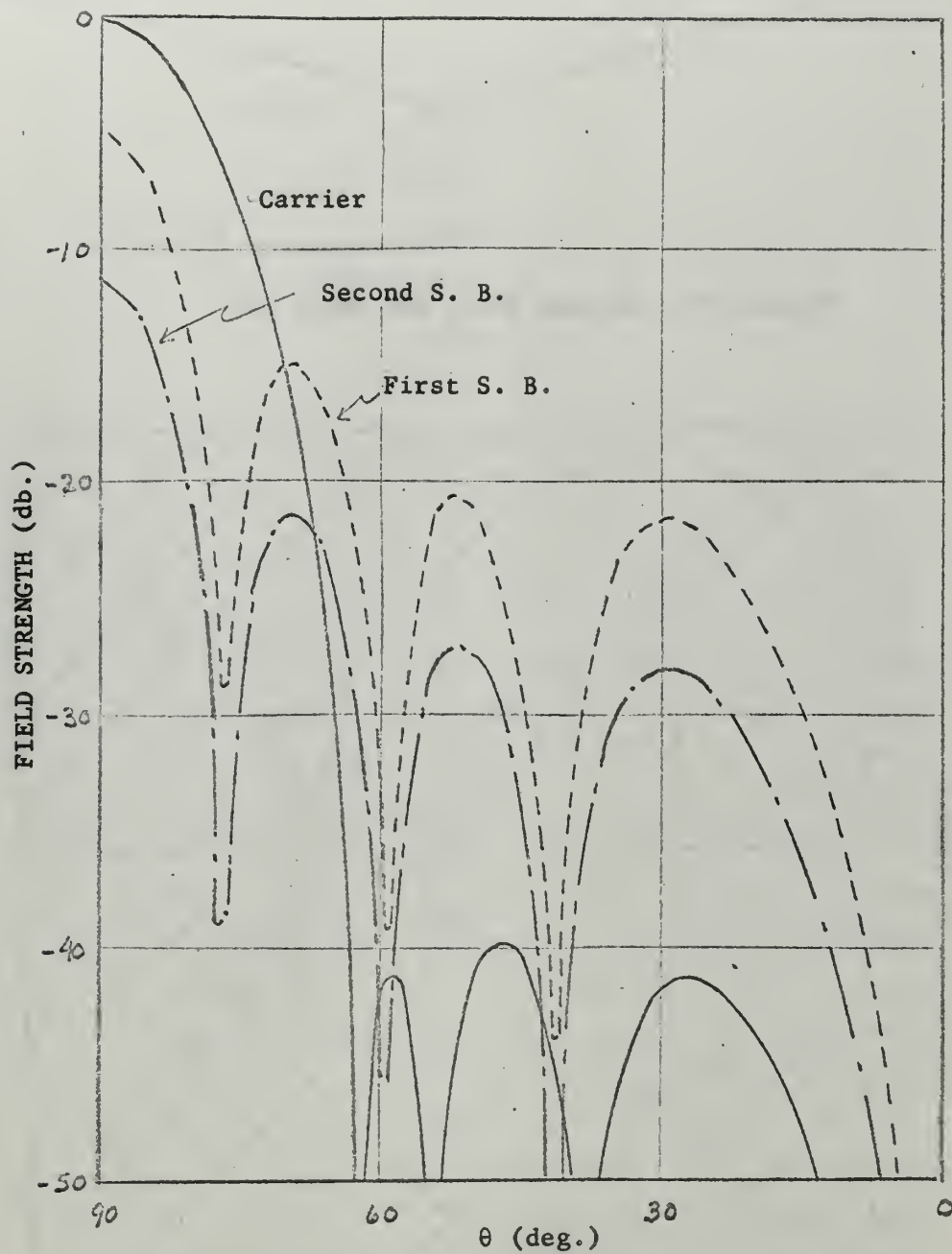


Figure 18. Array field patterns at the carrier and first two sideband frequencies for Model III with a 40 db. Dolph-Tchebyscheff distribution of  $\mu_{on}$ :  $C=0.25$ ,  $\phi_1=\phi_8=39.25^\circ$ ,  $\phi_2=\phi_7=28.0^\circ$ ,  $\phi_3=\phi_6=12.75^\circ$ , and  $\phi_4=\phi_5=0.0^\circ$



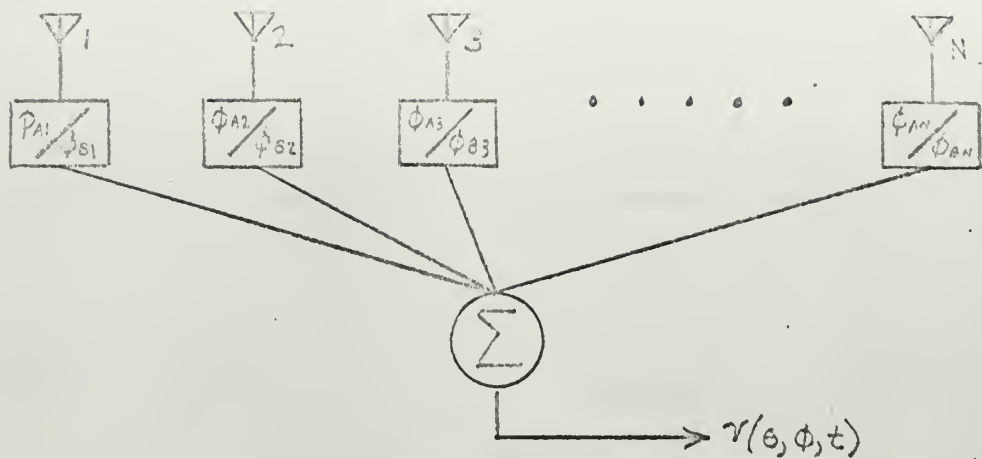


Figure 19. Antenna array for Model IV.

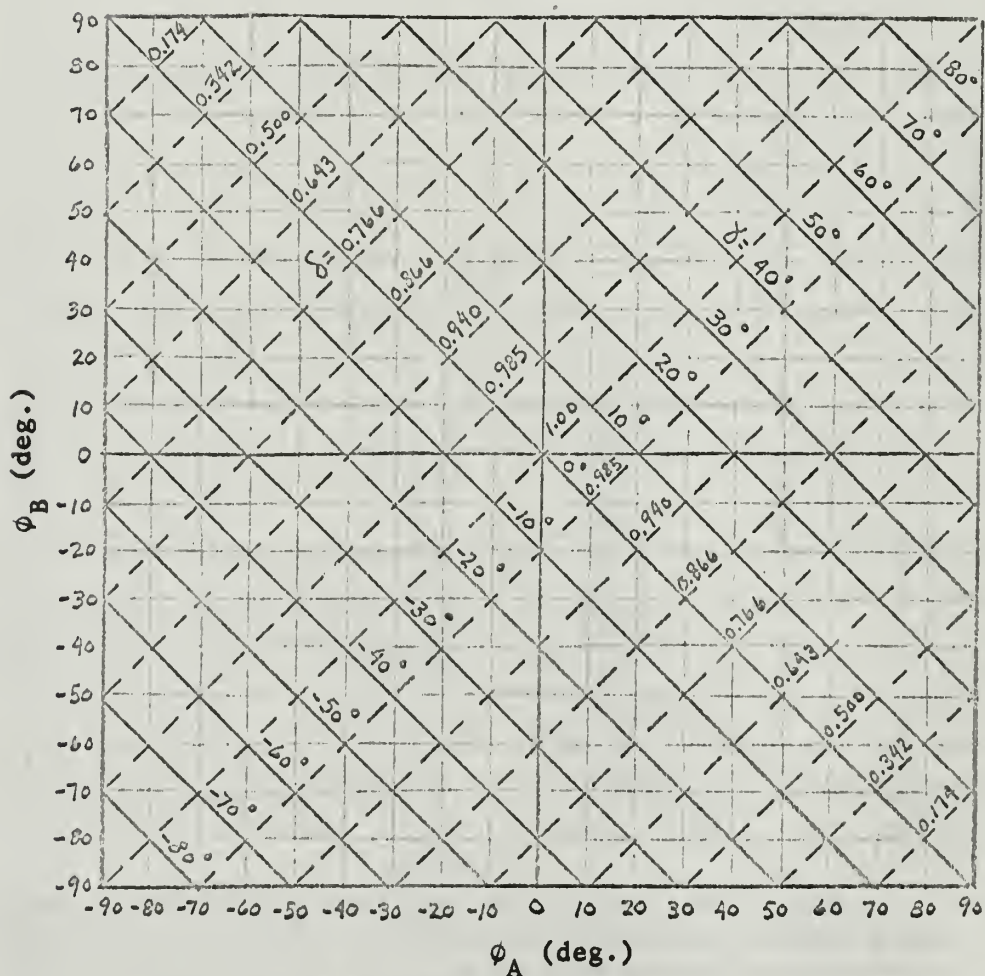


Figure 20. Nomogram for finding  $\delta \angle \gamma$  from  $\phi_A$  and  $\phi_B$ , and vice versa, using the relationship:

$$\delta \angle \gamma = \cos\left(\frac{\phi_A - \phi_B}{2}\right) \left[ \cos\left(\frac{\phi_A + \phi_B}{2}\right) + j \sin\left(\frac{\phi_A + \phi_B}{2}\right) \right]$$

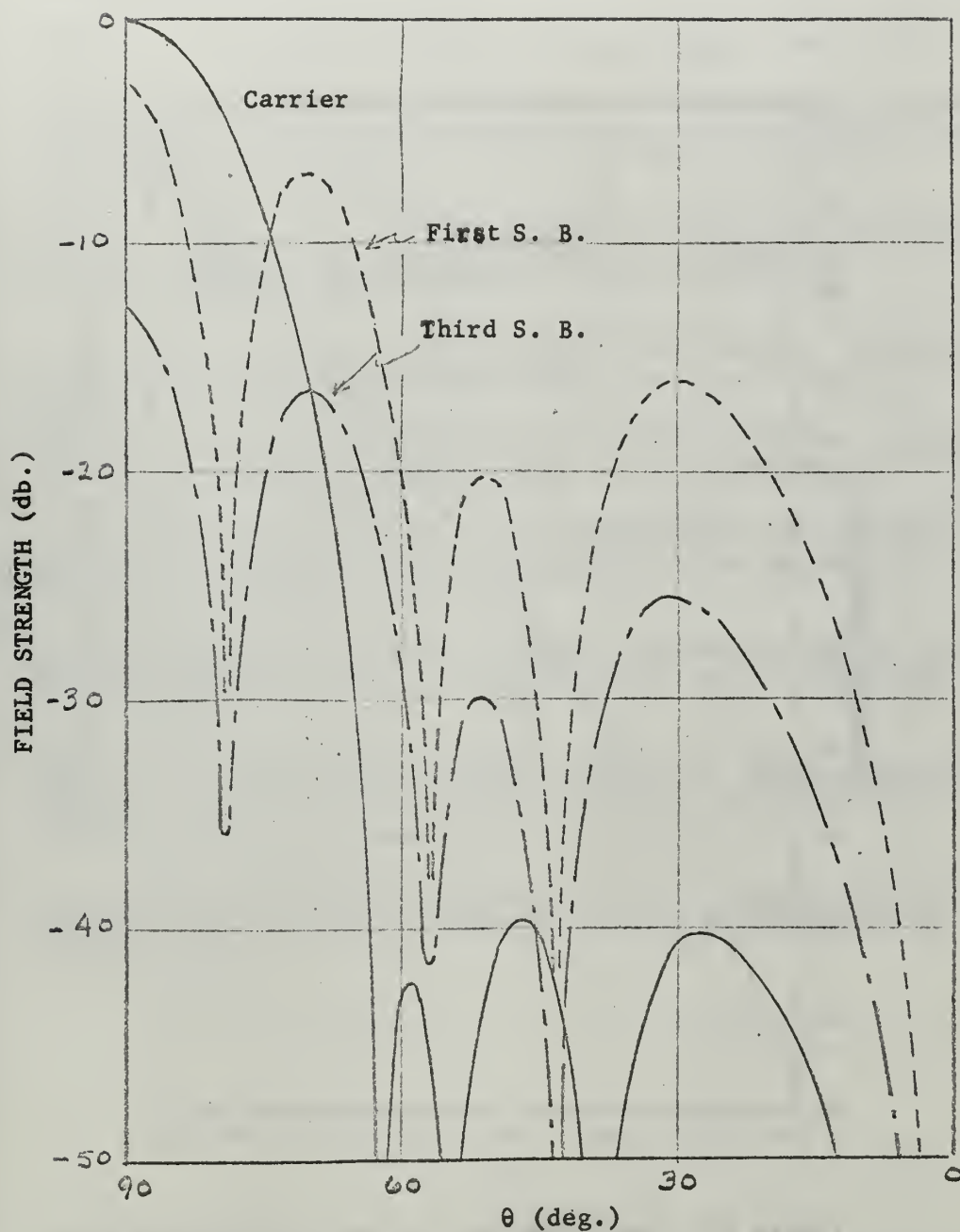


Figure 21. Array field patterns at the carrier and first and third sideband frequencies for Model IV with a 40 db. Dolph-Tchebyscheff distribution of  $A_{on}$ :  $\phi_{A1} = \phi_{A8} = -\phi_{B1} = -\phi_{B8} = 81.7^\circ$ ,  $\phi_{A2} = \phi_{A7} = -\phi_{B2} = -\phi_{B7} = 65.6^\circ$ ,  $\phi_{A3} = \phi_{A6} = -\phi_{B3} = -\phi_{B6} = 41.0^\circ$ , and  $\phi_{A4} = \phi_{A5} = \phi_{B4} = \phi_{B5} = 0.0^\circ$

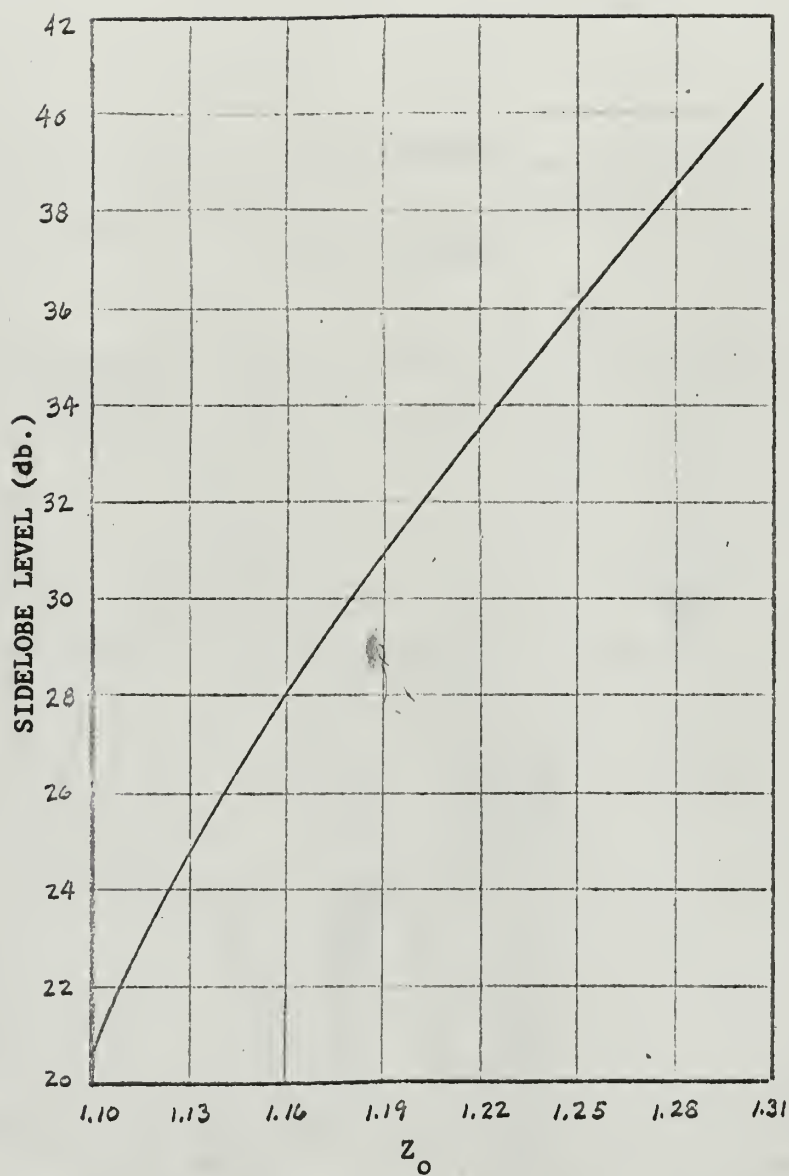


Figure 22. The parameter,  $Z_0$ , as a function of side-lobe level for an eight element Dolph-Tchebyscheff distribution.[4]

## BIBLIOGRAPHY

1. Kraus, J. D. Antennas. McGraw-Hill, 1950.
2. Schwartz, M. Information Transmissions, Modulation, and Noise. McGraw-Hill, 1959.
3. Silver, S. Microwave Antenna Theory and Design. McGraw-Hill, 1949.
4. Dolph, C. L. A current distribution for broadside arrays which optimizes the relationship between beam width and sidelobe level. Proceedings of the I.R.E., v. 34, June, 1946: 335-348.
5. Kummer, W. H., et al. Ultra-low sidelobes from time-modulated arrays. IEEE Transactions on Antennas and Propagation, v. AP-11, No. 6, November, 1963: 633-639.
6. \_\_\_\_\_, et al. Scanning without phase shifters. Electronics, v. 36, No. 13, 29 March 1963: 27-32.
7. Shanks, H. E. A new technique for electronic scanning. IRE Transactions on Antennas and Propagation, v. AP-9, March, 1961: 162-166.
8. \_\_\_\_\_, and R. W. Bickmore. Four-dimensional electromagnetic radiators. Canadian Journal of Physics, v. 37, March, 1959: 263-275.
9. Hougardy, H. H. Time domain sidelobe suppression. Hughes Research Laboratories. Final Report RADC-TR-60-112; AF 30-(602)-2021. 15 April 1960.
10. Kummer, W. H. Time domain antenna techniques. Hughes Aircraft Company. Technical Note RADC-TDR-61-290; AF 30-(602)-2410. October, 1961.
11. \_\_\_\_\_. Time domain antenna techniques. Hughes Aircraft Company. Technical Report RADC-TDR-62-153; AF 30-(602)-2410. January, 1962.



## APPENDIX

### THE DOLPH-TCHEBYSCHIEFF DISTRIBUTION

The Dolph-Tchebyscheff distribution is, in effect, a compromise between the uniform and the binomial distributions. A uniformly excited element distribution produces a field pattern with a relatively narrow beam width but with a high sidelobe level. The binomial distribution results in a pattern with zero sidelobes but with a very wide beam width. With the Dolph-Tchebyscheff distribution, the beam is widened somewhat and the sidelobe level is not zero; however, the relationship between the two is optimized.[1]

The theory behind the distributions has been covered in great detail throughout technical literature and as such, will not be repeated here.[1, 3, 4] Of interest in this study is the determination of the actual coefficient values associated with the distribution for an assumed eight element array. A plot of the sidelobe level as a function of the parameter  $Z_0$  is shown in Figure 22, p. 70, for an eight element array.[4] The graph is entered with the desired sidelobe level to obtain a value of the corresponding  $Z_0$ . This value of  $Z_0$  is then used in the following set of equations to solve for the required coefficients:

$$I_1 = I_8 = Z_0^7$$

$$I_2 = I_7 = 7I_1 - 7Z_0^5$$

$$I_3 = I_6 = 5I_2 - 14I_1 + 14Z_0^3$$

$$I_4 = I_5 = 3I_3 - 5I_2 + 7I_1 - 7Z_0$$



For example, assuming that the maximum desired sidelobe level is 40 db. below the main beam, Figure 22 gives the required value of  $Z_0$  as 1.30. This gives:

$$I_1 = I_8 = Z_0^7 = (1.30)^7 = 6.27$$

$$\begin{aligned} I_2 = I_7 &= 7I_1 - 7Z_0^5 \\ &= 7(6.27) - 7(1.30)^5 = 18.00 \end{aligned}$$

$$\begin{aligned} I_3 = I_6 &= 5I_2 - 14I_1 + 14Z_0^3 \\ &= 5(18.00) - 14(6.27) + 14(1.30)^3 \\ &= 32.90 \end{aligned}$$

$$\begin{aligned} I_4 = I_5 &= 3I_3 - 5I_2 + 7I_1 - 7Z_0 \\ &= 3(32.90) - 5(18.00) + 7(6.27) - 7(1.30) \\ &= 43.55 \end{aligned}$$

If these coefficients are now normalized such that

$$I_4 = I_5 = 1.000$$

the desired distribution is

$$I_1 = I_8 = \frac{6.27}{43.55} = 0.144$$

$$I_2 = I_7 = \frac{18.00}{43.55} = 0.413$$

$$I_3 = I_6 = \frac{32.90}{43.55} = 0.755$$

$$I_4 = I_5 = 1.000$$

The Dolph-Tchebyscheff distribution was originally developed for the purpose of scaling the magnitude of the excitations in the individual elements of an array. In the modulating techniques under investigation in this study, the distribution was applied to the expressions for the field pattern of the antenna. As such, the coefficients governed such factors

as the element ON times, the frequency of modulation, or the phase relationship between the elements as required by the particular type of modulation.


# INITIAL DISTRIBUTION LIST

	No. Copies
1. Defense Documentation Center Cameron Station Alexandria, Virginia 22314	20
2. Library U. S. Naval Postgraduate School, Monterey, California	2
3. Commandant, U. S. Coast Guard (OC) U. S. Coast Guard Headquarters Washington, D. C.	1
4. Prof Paul E. Cooper (Thesis Advisor) Department of Electrical Engineering U. S. Naval Postgraduate School, Monterey, California	1
5. LT Stephen Patrick Leane, USCG 1022 Del Monte Blvd. Pacific Grove, California 93950	1



DOCUMENT CONTROL DATA - R&D

(Security classification of title, body of abstract and indexing annotation must be entered when the overall report is classified)

1. ORIGINATING ACTIVITY (Corporate author)  U. S. Naval Postgraduate School Monterey, California		2a. REPORT SECURITY CLASSIFICATION  Unclassified	
		2b. GROUP	
3. REPORT TITLE  A DESIGN STUDY OF ANTENNA MODULATION TECHNIQUES RESULTING IN REDUCED SIDELobe LEVELS			
4. DESCRIPTIVE NOTES (Type of report and inclusive dates)  Thesis, December 1966			
5. AUTHOR(S) (Last name, first name, initial)  Leane, Stephen P., Lieutenant, U. S. Coast Guard			
6. REPORT DATE  December 1966		7a. TOTAL NO. OF PAGES  75	7b. NO. OF REFS  11
8a. CONTRACT OR GRANT NO.  b. PROJECT NO.  c.  d.		9a. ORIGINATOR'S REPORT NUMBER(S)  9b. OTHER REPORT NO(S) (Any other numbers that may be assigned this report)	
10. AVAILABILITY/LIMITATION NOTICES  		This document has been approved for public release and sale; its distribution is unlimited.  #1 Memorandum 12/22/69	
11. SUPPLEMENTARY NOTES		12. SPONSORING MILITARY ACTIVITY	
13. ABSTRACT  It is desirable, for many applications, to utilize a receiving antenna system which is sensitive only to radiation from a specific direction. In order to eliminate the incoming signals from all other directions, the side-lobe strength in these regions must be significantly lower than the main beam. Time modulation was applied to certain of the antenna's parameters in an effort to reduce the sidelobe level of a linear receiving antenna array. Such factors as the effective length of the array, and the frequency and phase of the signals received by each of the individual elements were periodically varied in time. After summing the voltage contribution from each element, the resultant signal was suitably filtered and sent to the detector. Antenna field patterns were developed in mathematical terms and the experimental calculations were made on the CDC 1604 computer. For all forms of modulation investigated, it was possible to reduce the sidelobe strength by more than an order of magnitude below the unmodulated level.			



14. KEY WORDS	LINK A		LINK B		LINK C	
	ROLE	WT	ROLE	WT	ROLE	WT
Antenna array Sidelobe reduction Antenna modulation						

### INSTRUCTIONS

1. **ORIGINATING ACTIVITY:** Enter the name and address of the contractor, subcontractor, grantee, Department of Defense activity or other organization (*corporate author*) issuing the report.

2a. **REPORT SECURITY CLASSIFICATION:** Enter the overall security classification of the report. Indicate whether "Restricted Data" is included. Marking is to be in accordance with appropriate security regulations.

2b. **GROUP:** Automatic downgrading is specified in DoD Directive 5200.10 and Armed Forces Industrial Manual. Enter the group number. Also, when applicable, show that optional markings have been used for Group 3 and Group 4 as authorized.

3. **REPORT TITLE:** Enter the complete report title in all capital letters. Titles in all cases should be unclassified. If a meaningful title cannot be selected without classification, show title classification in all capitals in parenthesis immediately following the title.

4. **DESCRIPTIVE NOTES:** If appropriate, enter the type of report, e.g., interim, progress, summary, annual, or final. Give the inclusive dates when a specific reporting period is covered.

5. **AUTHOR(S):** Enter the name(s) of author(s) as shown on or in the report. Enter last name, first name, middle initial. If military, show rank and branch of service. The name of the principal author is an absolute minimum requirement.

6. **REPORT DATE:** Enter the date of the report as day, month, year; or month, year. If more than one date appears on the report, use date of publication.

7a. **TOTAL NUMBER OF PAGES:** The total page count should follow normal pagination procedures, i.e., enter the number of pages containing information.

7b. **NUMBER OF REFERENCES:** Enter the total number of references cited in the report.

8a. **CONTRACT OR GRANT NUMBER:** If appropriate, enter the applicable number of the contract or grant under which the report was written.

8b, 8c, & 8d. **PROJECT NUMBER:** Enter the appropriate military department identification, such as project number, subproject number, system numbers, task number, etc.

9a. **ORIGINATOR'S REPORT NUMBER(S):** Enter the official report number by which the document will be identified and controlled by the originating activity. This number must be unique to this report.

9b. **OTHER REPORT NUMBER(S):** If the report has been assigned any other report numbers (*either by the originator or by the sponsor*), also enter this number(s).

10. **AVAILABILITY/LIMITATION NOTICES:** Enter any limitations on further dissemination of the report, other than those

imposed by security classification, using standard statements such as:

- (1) "Qualified requesters may obtain copies of this report from DDC."
- (2) "Foreign announcement and dissemination of this report by DDC is not authorized."
- (3) "U. S. Government agencies may obtain copies of this report directly from DDC. Other qualified DDC users shall request through \_\_\_\_\_."
- (4) "U. S. military agencies may obtain copies of this report directly from DDC. Other qualified users shall request through \_\_\_\_\_."
- (5) "All distribution of this report is controlled. Qualified DDC users shall request through \_\_\_\_\_."

If the report has been furnished to the Office of Technical Services, Department of Commerce, for sale to the public, indicate this fact and enter the price, if known.

11. **SUPPLEMENTARY NOTES:** Use for additional explanatory notes.

12. **SPONSORING MILITARY ACTIVITY:** Enter the name of the departmental project office or laboratory sponsoring (*paying for*) the research and development. Include address.

13. **ABSTRACT:** Enter an abstract giving a brief and factual summary of the document indicative of the report, even though it may also appear elsewhere in the body of the technical report. If additional space is required, a continuation sheet shall be attached.

It is highly desirable that the abstract of classified reports be unclassified. Each paragraph of the abstract shall end with an indication of the military security classification of the information in the paragraph, represented as (TS), (S), (C), or (U).

There is no limitation on the length of the abstract. However, the suggested length is from 150 to 225 words.

14. **KEY WORDS:** Key words are technically meaningful terms or short phrases that characterize a report and may be used as index entries for cataloging the report. Key words must be selected so that no security classification is required. Identifiers, such as equipment model designation, trade name, military project code name, geographic location, may be used as key words but will be followed by an indication of technical context. The assignment of links, roles, and weights is optional.







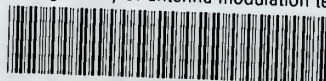






thesL354

A design study of antenna modulation tec



3 2768 001 03149 5

DUDLEY KNOX LIBRARY